Commissioning Status of High Luminosity Collider Rings for SuperKEKB

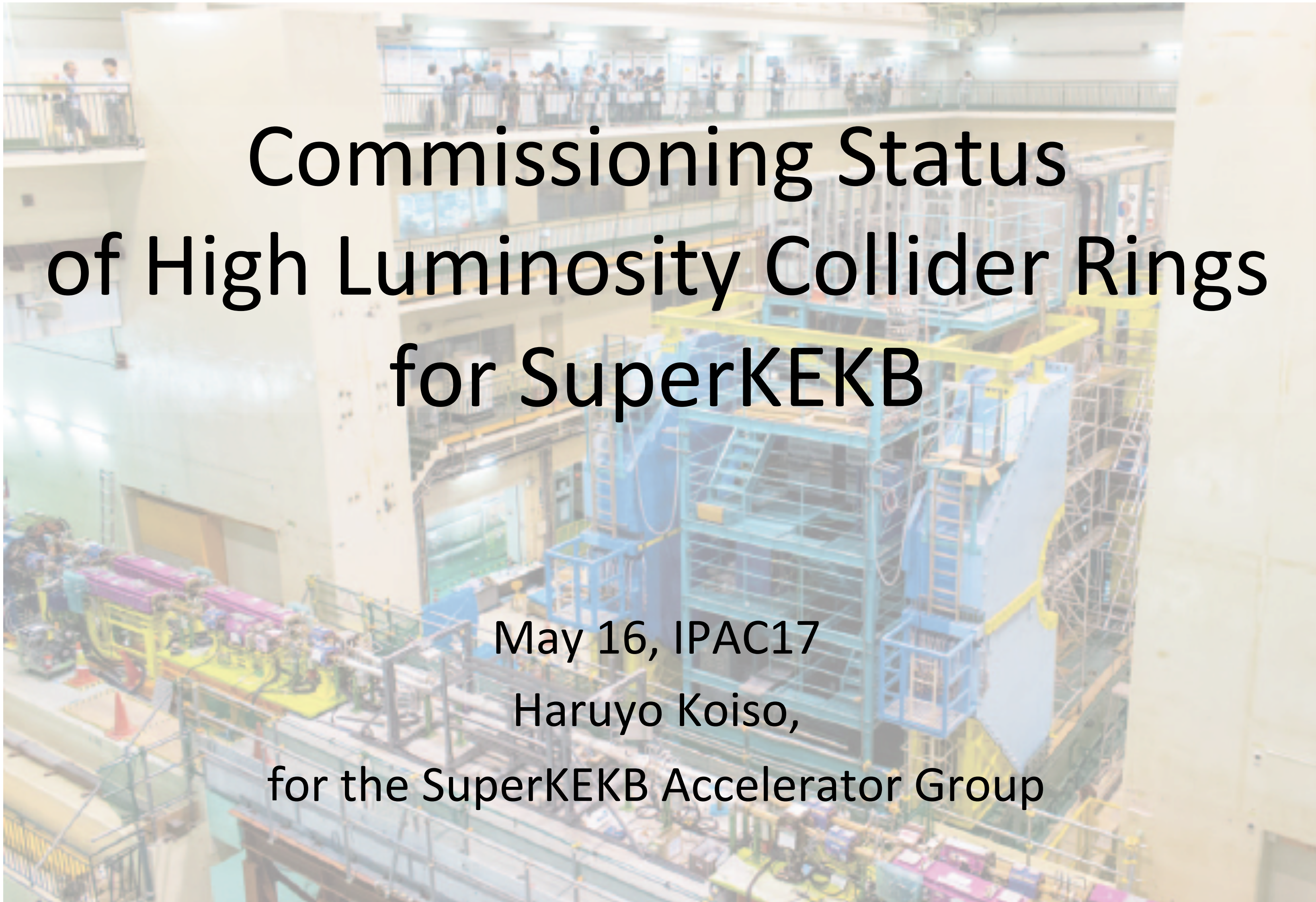

May 16, IPAC17

Haruyo Koiso,

for the SuperKEKB Accelerator Group

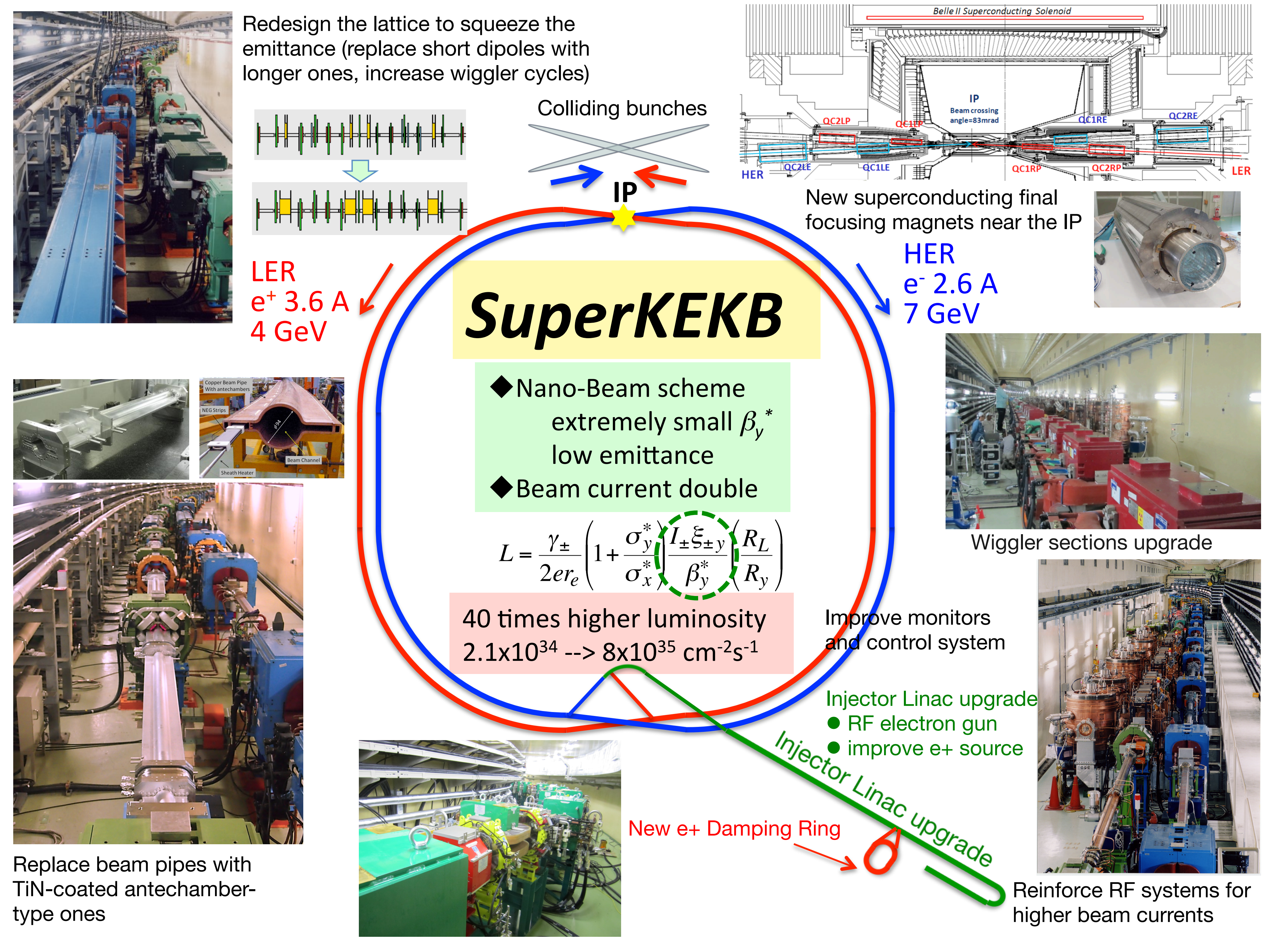
Redesign the lattice to squeeze the emittance (replace short dipoles with longer ones, increase wiggler cycles)
Colliding bunches
IP
Belle II Superconducting Solenoid
IP
Beam crossing angle=83mrad
QC2LP
QC1LP
QC1RE
QC2RE
HER
QC2LE
QC1LE
QC1RP
QC2RP
LER
New superconducting final focusing magnets near the IP
LER
e^+ 3.6 A
4 GeV
HER
e^- 2.6 A
7 GeV
SuperKEKB
◆Nano-Beam scheme
extremely small β_y^*
low emittance
◆Beam current double
$L = \frac{\gamma_\pm}{2er_e}\left(1+\frac{\sigma_y^*}{\sigma_x^*}\right)\left(\frac{I_\pm \xi_{\pm y}}{\beta_y^*}\right)\left(\frac{R_L}{R_y}\right)$
40 times higher luminosity
2.1×10^{34} --> 8×10^{35} $cm^{-2}s^{-1}$
Copper Beam Pipe With antechambers
NEG Strips
Beam Channel
Sheath Heater
Wiggler sections upgrade
Improve monitors and control system
Injector Linac upgrade
● RF electron gun
● improve e+ source
Injector Linac upgrade
New e+ Damping Ring
Replace beam pipes with TiN-coated antechamber-type ones
Reinforce RF systems for higher beam currents

SuperKEKB

Beam energy (LER/HER) : 3.5/8.0 GeV (KEKB) → **4.0/7.0** GeV (SuperKEKB)

Beam current (LER/HER):

1.64/1.19 A (KEKB)

→ **3.6/2.6 A** (SuperKEKB)

Beam-beam parameter:

0.129/0.090 (KEKB)

→ **0.088/0.081** (SuperKEKB)

Lorentz factor

$$L = \frac{\gamma_{\pm}}{2er_e}\left(1+\frac{\sigma_y^*}{\sigma_x^*}\right)\frac{I_{\pm}\xi_{\pm y}}{\beta_y^*}\left(\frac{R_L}{R_y}\right)$$

Classical electron radius

Beam size ratio

Geometrical reduction factors due to crossing angle and hour-glass effect

Luminosity:

2.11 $\times 10^{34}$ $cm^{-2}s^{-1}$ (KEKB)

→ **80 $\times 10^{34}$ $cm^{-2}s^{-1}$** (SuperKEKB)

Vertical β at the IP:

5.9/5.9 mm (KEKB)

→ **0.27/0.3 mm** (SuperKEKB)

Challenging

SuperKEKB

Nano-beam scheme

Short longitudinal size of overlap region
in order to squeeze β^*_y avoiding the hourglass effect.

Small ϕ_{Piw}

KEKB : ~ 1
(θ_x=11 mrad)

Large ϕ_{Piw}

SuperKEKB : ~ 20
(θ_x=41.5 mrad)

d ~ σ_z/20

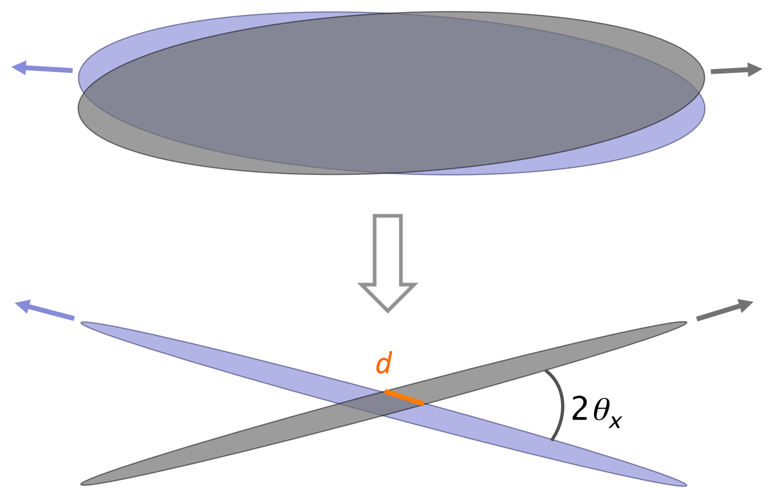

θ_x: half crossing angle

Piwinski Angle

$$\phi_{Piw} = \frac{\theta_x \sigma_z}{\sigma^*_x}$$

Longitudinal overlap region

$$d = \frac{\sigma^*_x}{\theta_x} = \frac{\sigma_z}{\phi_{Piw}}$$

Proposed by P. Raimondi
together with Crab Waist.

SuperKEKB

Beam commissioning will be performed in three phases.

~5 months
Feb. - June 2016
finished

Phase 1
w/o QCS and Belle II

basic machine tuning
vacuum scrubbing

~5 months

Phase 2
w/QCS and Belle II
w/o Vertex detector

Luminosity tuning
Target luminosity:
$1 \times 10^{34}\ cm^{-2}\ s^{-1}$
background study

Phase 3
Physics Run

Luminosity tuning
Target luminosity:
$8 \times 10^{35}\ cm^{-2}\ s^{-1}$

Here we are.

QCS: final-focus superconducting magnet system

Y. Funakoshi et al.

Phase-1 Commissioning

Phase 1 milestones: Feb. to June, 2016
- Feb. 1: BT tuning started
- Feb. 8: LER injection tuning started
- Feb. 10: beam storage in LER
- Feb. 22: HER injection tuning started
- Feb. 26: beam storage in HER

Tasks during phase 1 operation
- Basic machine tuning
- Vacuum scrubbing
- Low emittance tuning
- Machine studies on electron cloud effect, beam background, etc.

Achieved beam current
870 mA (HER)
1010 mA (LER)

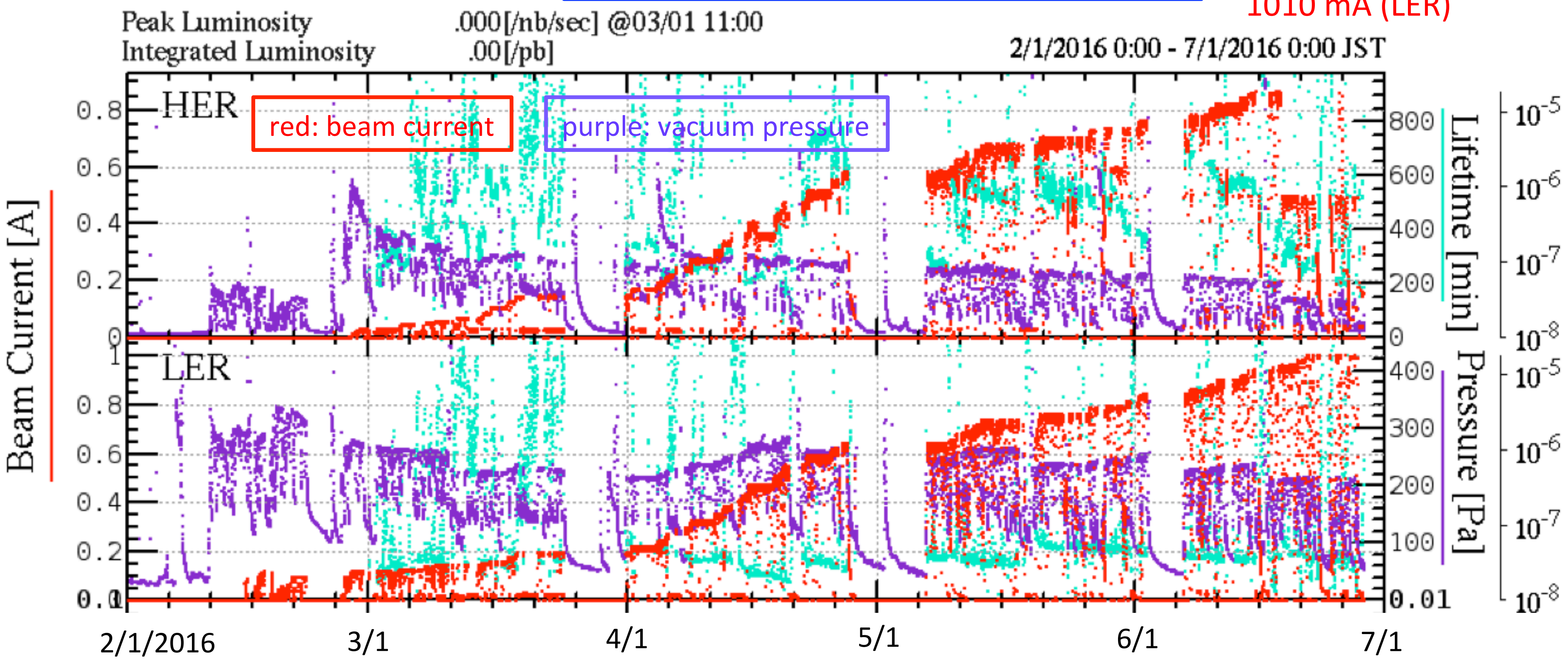

K. Akai

Vacuum Scrubbing

- The vacuum system worked well with newly introduced components.
- Integrated beam currents satisfied requirement for Belle II roll-in.

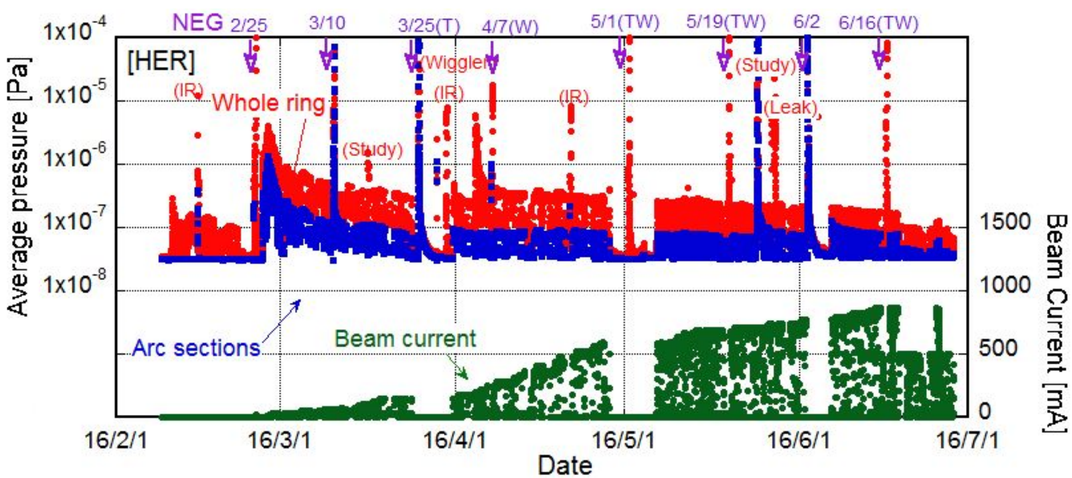

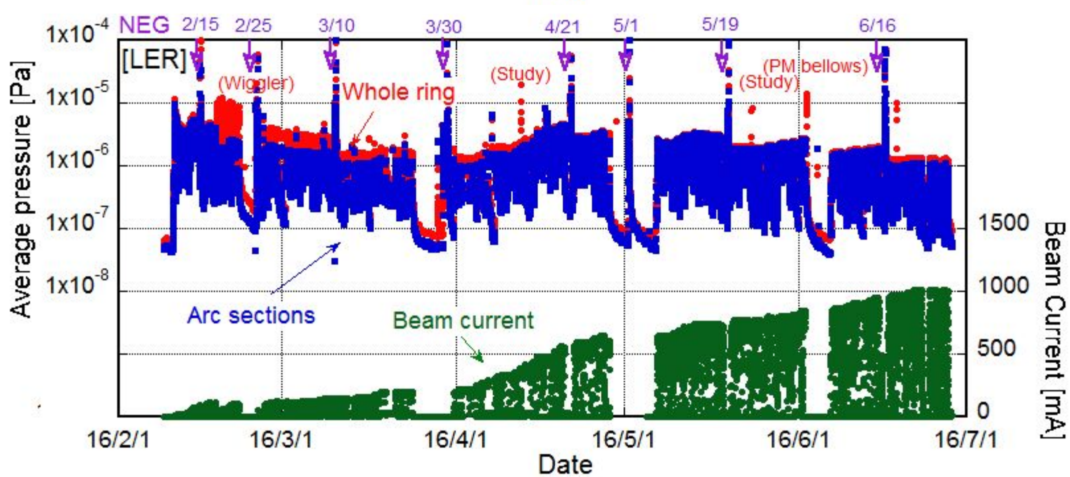

[HER]

- Base pressure: ~3×10^{-8} Pa
- Max. beam current: 870 mA
- Int. beam current: 660 Ah
- Avg. Pressure: ~ 2×10^{-7} Pa
  (arc sections) ~ 6×10^{-8} Pa
- Lifetime ~ 400 min.

[LER]

- Base pressure: ~5×10^{-8} Pa
- Max. beam current: 1010 mA
- Int. beam current: 780 Ah
- Avg. Pressure: ~ 1×10^{-6} Pa
- Lifetime: ~ 70 min.
  (with Emittance control Knob ON)

Y. Suetsugu et al.

Vacuum Scrubbing

- Vacuum Scrubbing was performed smoothly.
  - Photon-stimulated desorption coefficient η decreased to ~5x10^{-6} molecules photon^{-1} in LER and to less than 1x10^{-7} in HER because >80% of HER chambers were reused (Memory effect).

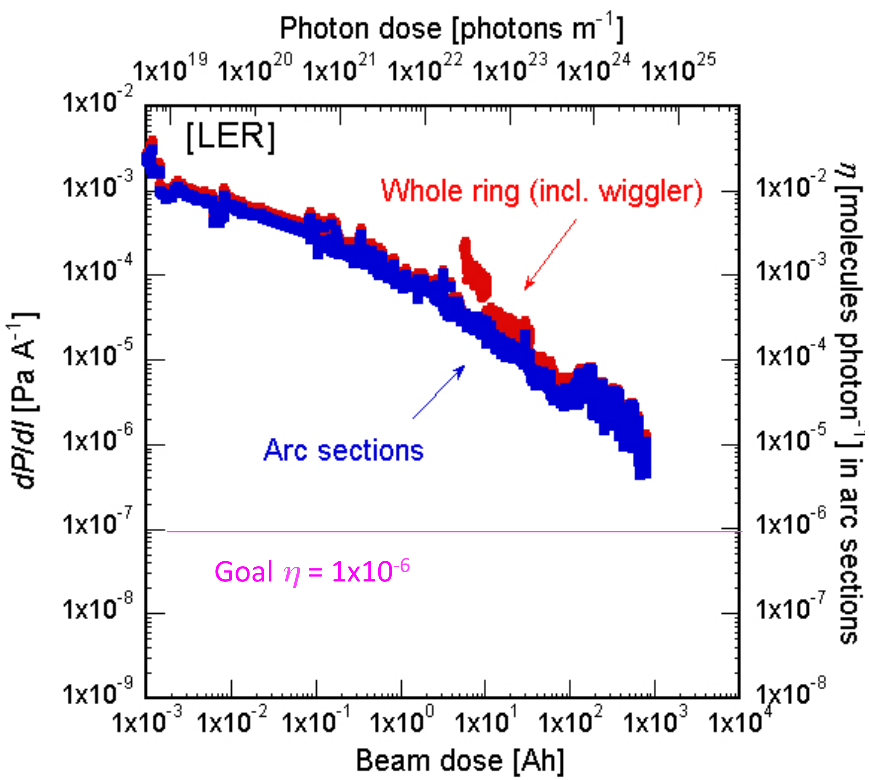

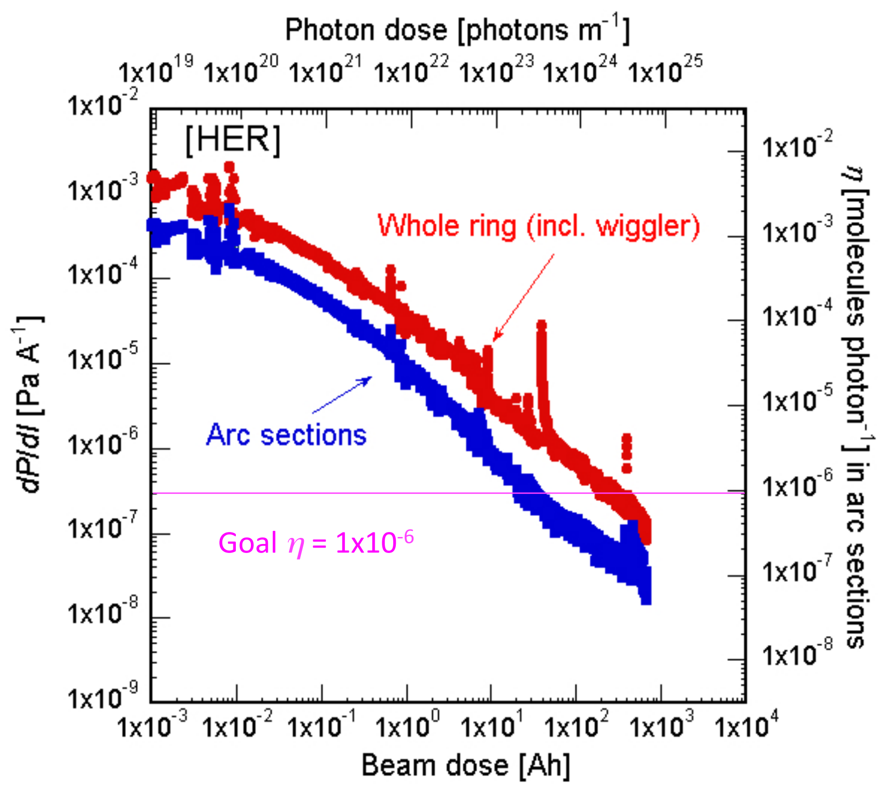

Y. Suetsugu et al.

Electron Cloud Effect

- Electron cloud instability can be a serious problem for LER (e^+).
  - Blowup of vertical beam size deteriorates the luminosity.
- For the SuperKEKB, the threshold of electron density to excite the head-tail instability n_e is estimated to be $2\text{-}3 \times 10^{11}\ e^- \ m^{-3}$.
- Various mitigation techniques were adopted in the SuperKEKB.
  - Antechambers
  - TiN coating
  - Solenoid field (not yet)
  - Clearing electrode (w)
  - Grooved surface (B)

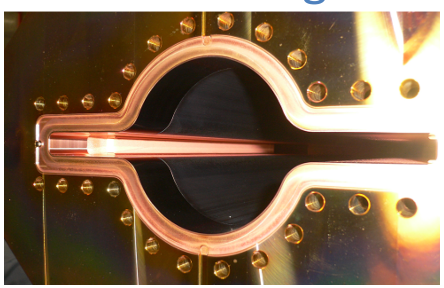

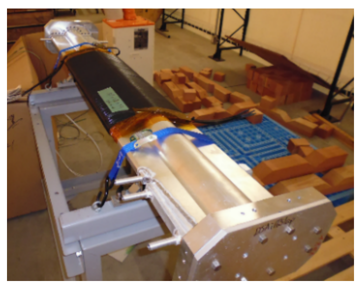
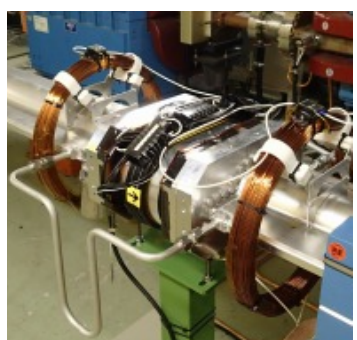
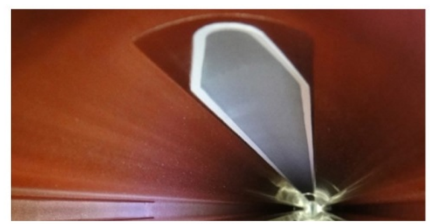
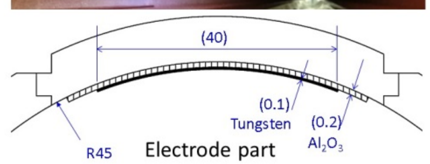

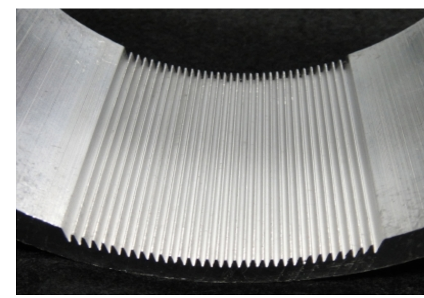
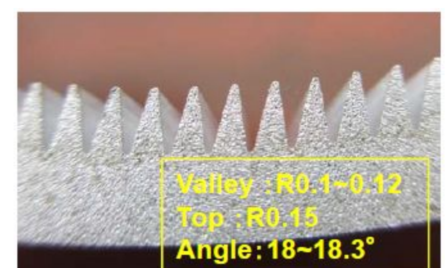

Y. Suetsugu et al.

Electron Cloud Effect

- Countermeasures in SuperKEKB LER (Final configuration*)

Sections	L [m]	L [%]	Countermeasure	Material
Total	3016	100		
Drift space (arc)	1629 m	54	TiN coating + Solenoid	Al (arc)
Steering mag.	316 m	10	TiN coating + Solenoid	Al
Bending mag.	519 m	17	TiN coating + Grooved surface	Al
Wiggler mag.	154 m	5	Clearing Electrode	Cu
Q & SX mag.	254 m	9	TiN coating	Al (arc)
RF section	124 m	4	(TiN coating +) Solenoid	Cu
IR section	20 m	0.7	(TiN coating +) Solenoid	Cu

*Solenoid coils are not yet installed.

With above countermeasures,
n_e ~2×10^{10} e^- m^{-3}
is expected.

Without solenoids,
n_e ~6×10^{11} e^- m^{-3}

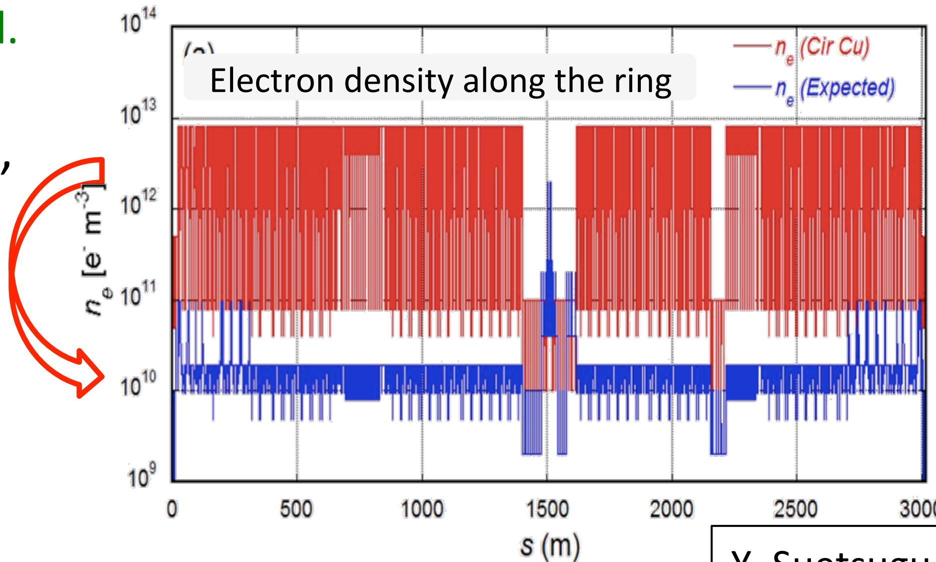

Y. Suetsugu et al.

Electron Cloud Effect

- Electron density was measured by electron current monitors in a drift space with and w/o TiN coating.
- Antechamber and TiN coating are well functioning.
- Electron current at aluminum with TiN coating is much lower than that without it.

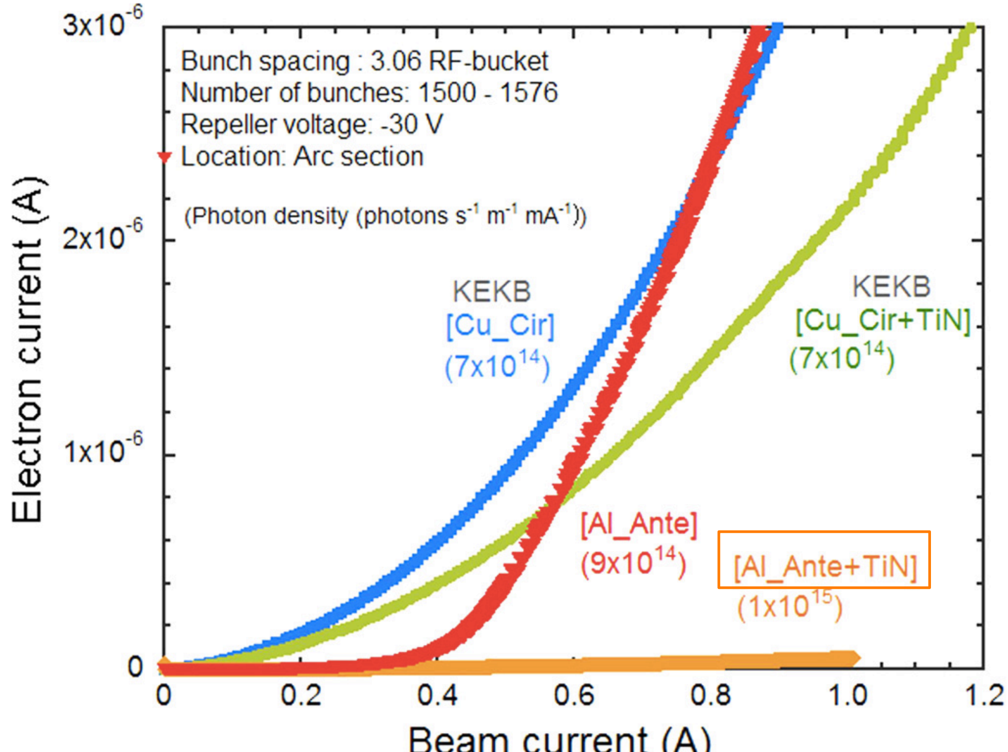

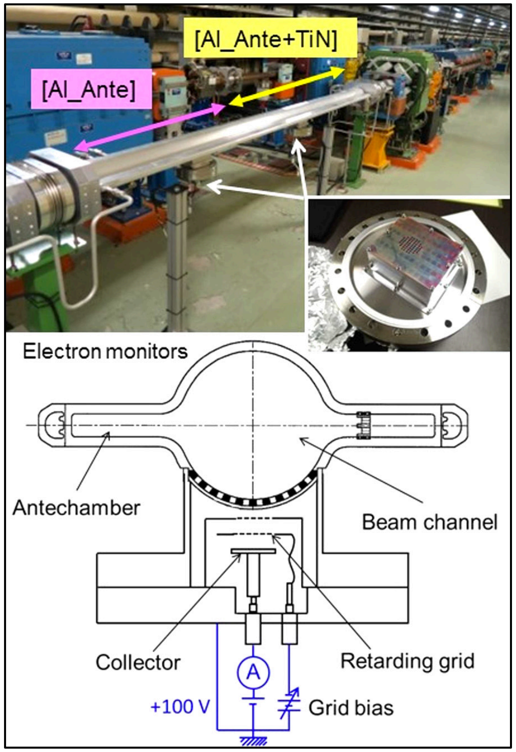

Y. Suetsugu et al, J. Vac. Sci. Technol. A 35, 03E103

Y. Suetsugu et al.

Electron Cloud Effect

- Electron cloud effect was firstly observed at ~ 0.6 A.
  - Nonlinear pressure rise and vertical beam size blowup, etc.
  - Caused by the electrons in Al-alloy bellows chambers without TiN coating. Total length was 5% of the ring (0.2 m x ~830), but the electron density was very high there.
  - Permanent magnets making axial magnetic field (~100 G) were attached to all of Al bellows.
- Nonlinear pressure rise and beam size blowup relaxed. However they are still observed at higher current.

Al bellows in tunnel

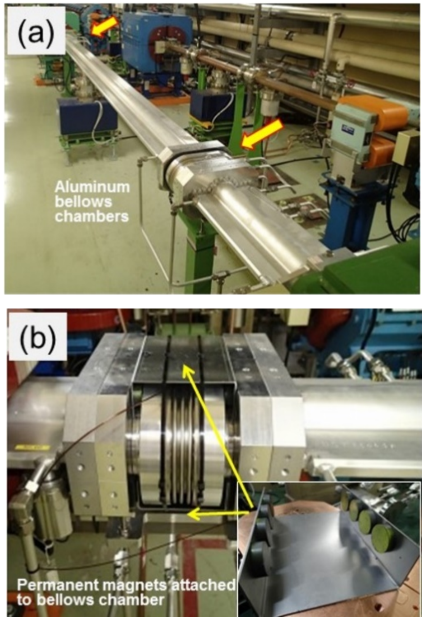

Vertical beam size blowup

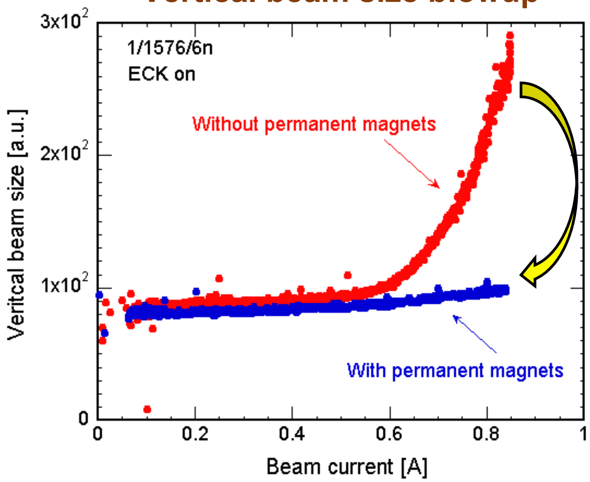

Nonlinear pressure rise

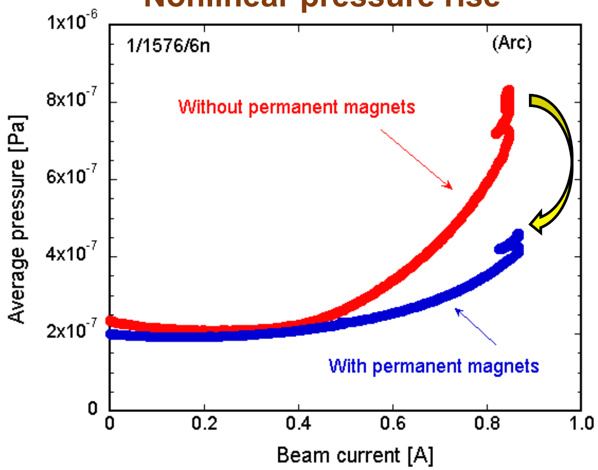

Permanent magnets

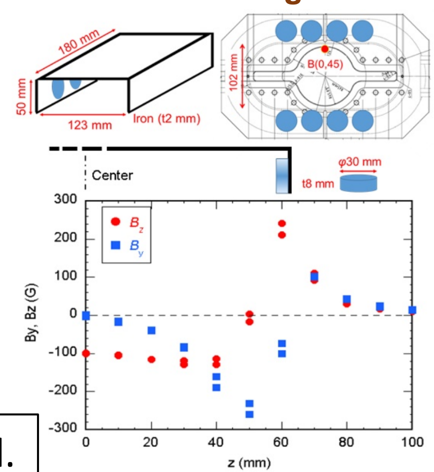

Y. Suetsugu et al.

Electron Cloud Effect

- Threshold current of beam size blowup is almost proportional to the linear current density (bunch current / bunch spacing in RF bucket).
  - The beam size blowup occurs at almost same point in the linear current density.
  - The same behavior was observed at KEKB (Cu circular chamber without coating). Without axial magnetic fields, the threshold was 0.04 mA/bucket.

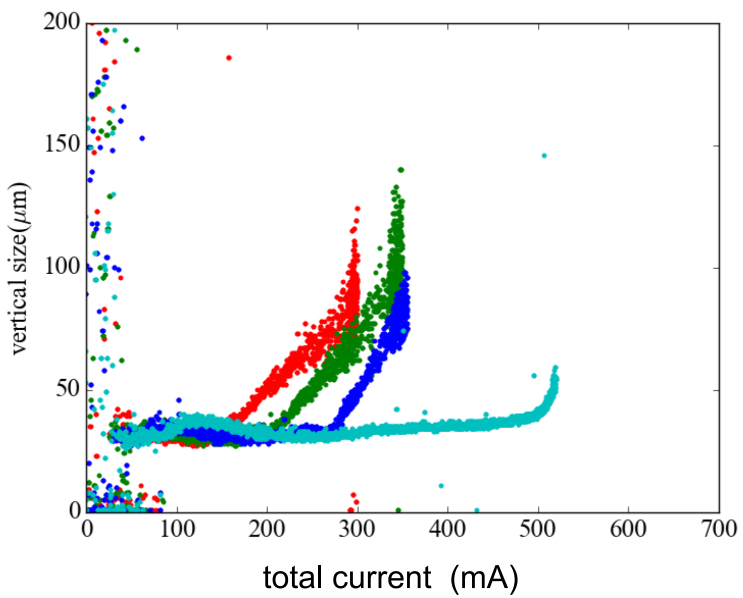

Ex. 4/150/3 : 4 trains, 150 bunches/train, 3 RF-bucket spacing

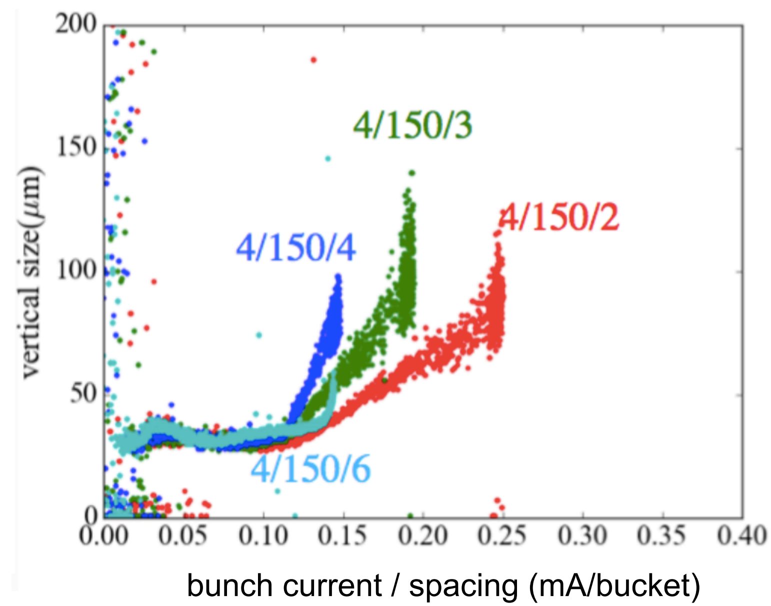

H. Fukuma et al.

Electron Cloud Effect

- Threshold of the beam size blowup increased from 0.10-0.12 to 0.18-0.20 mA/bucket after installation of the permanent magnets.
  - Our target is 0.72 mA/bucket. (3600 mA/2500 bunches/2 buckets spacing)

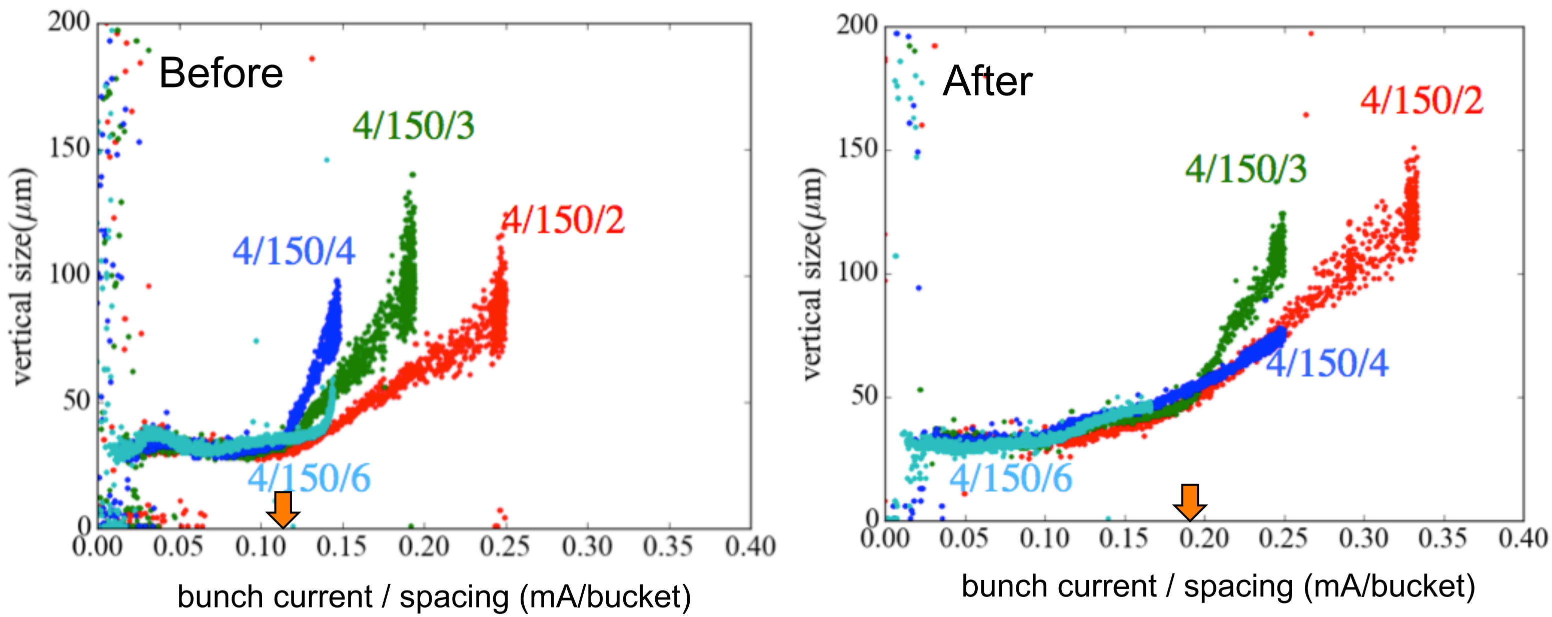

H. Fukuma et al.

Electron Cloud Effect

- Electron density in a drift space was estimated from measured by the electron current monitors.
- The electron density in the region w/o coating is higher by one order of magnitude.
- Around the blowup threshold, measured electron densities are not so different from simulation.

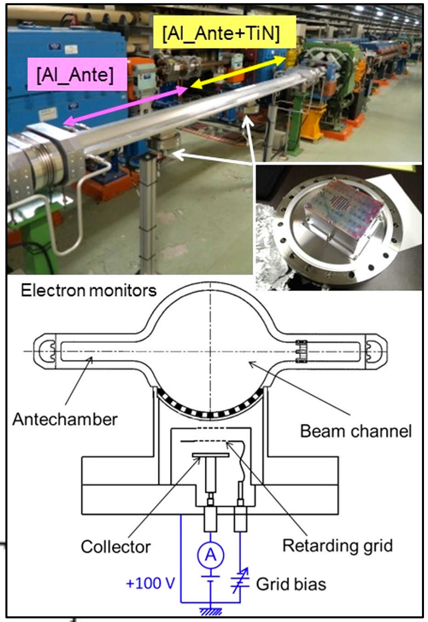

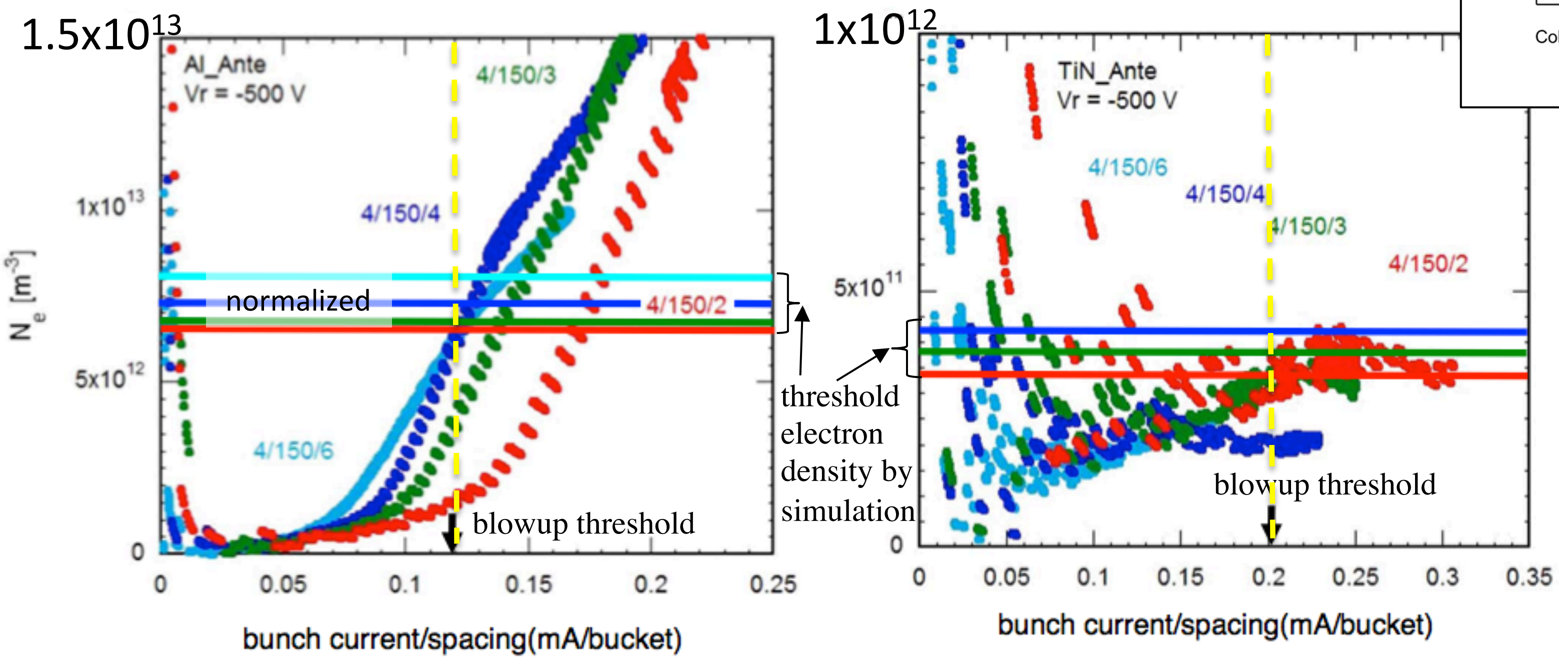

H. Fukuma et al.

Electron Cloud Effect

- Vertical sideband spectrum changed before and after the installation of permanent magnets, from drift mode to solenoid mode.
- The drift mode still appeared at high current after the installation in the case of 2 bucket spacing. This suggests that the electron clouds still remain in drift spaces.
- The blowup and the nonlinear pressure rise were still observed at higher current in the fill pattern 1/1576/3.06 for vacuum scrubbing.
- Pressure relaxed by attaching permanent magnets in drift spaces.
- **Permanent magnets will be attached to drift spaces all over the ring before Phase-2.**

Vertical sideband spectrum

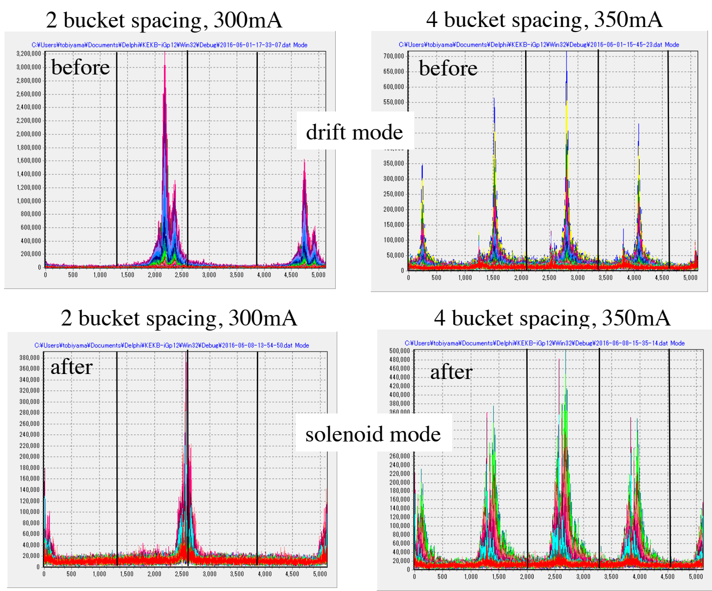

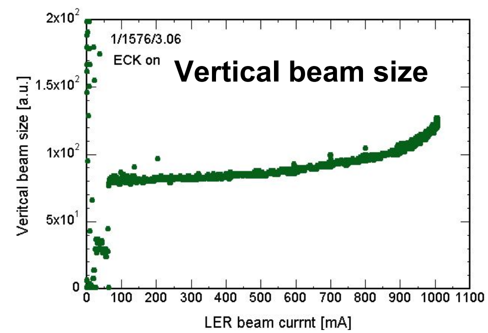

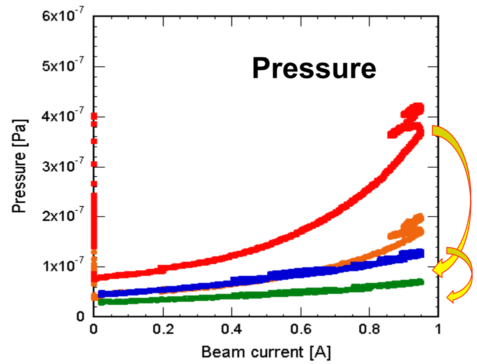

permanent magnets in drift spaces

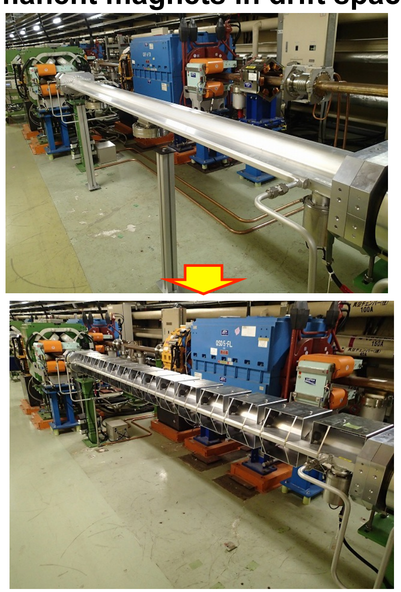

H. Fukuma, Y. Suetsugu et al.

Electron Cloud Effect

SEY

- The electron cloud was formed in the drift space with antechambers and TiN coating.
- The simulation of ECE indicates that the maximum SEY should be larger than an average of approximately 1.3 in the ring to excite the ECE in the present condition of LER.
- On the other hand, the maximum SEY measured in the laboratory was 0.9-1.2 at the estimated electron dose of 5 x 10^{-4} C mm^{-2}, where the incident electrons was 250 eV.
- The reason of the difference has not been clarified.

Possibilities:

- The dose of electrons with sufficient energies is still low.
- The pressure is still high in the beam pipe. In an experiment, the maximum SEY is high if the samples are not baked and the pressure in the test chamber is high.
- There is a place where the electron density is high. Al-alloy beam pipes without coating still remain in the straight section.

Further investigation in Phase-2.

Change of measured SEY against electron dose

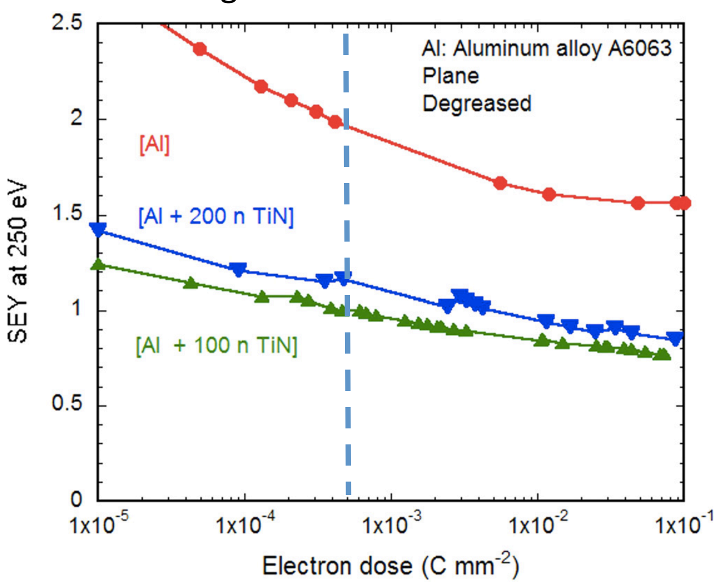

Y. Suetsugu et al, J. Vac. Sci. Technol. A 35, 03E103

Y. Suetsugu et al.

Electron Cloud Effect

- Antechamber and TiN coating are working well. Reduction of secondary electron by TiN coating is clearly observed.
- The electron clouds are still formed in drift spaces with antechambers and TiN coating.
- Permanent magnets will be attached to drift spaces all over the ring before Phase-2.
- More simulations on effect of installing permanent magnets are going on.
- Further studies on SEY will be performed in Phase-2.

Low Emittance Tuning

- Optics corrections have been worked successfully in both rings.
- Tentative target of vertical emittance has been achieved in LER.
- Measurements with X-ray monitor (XRM) give larger ε_y in HER.
  - More calibration of XRM and larger βy at RXM in Phase-2.

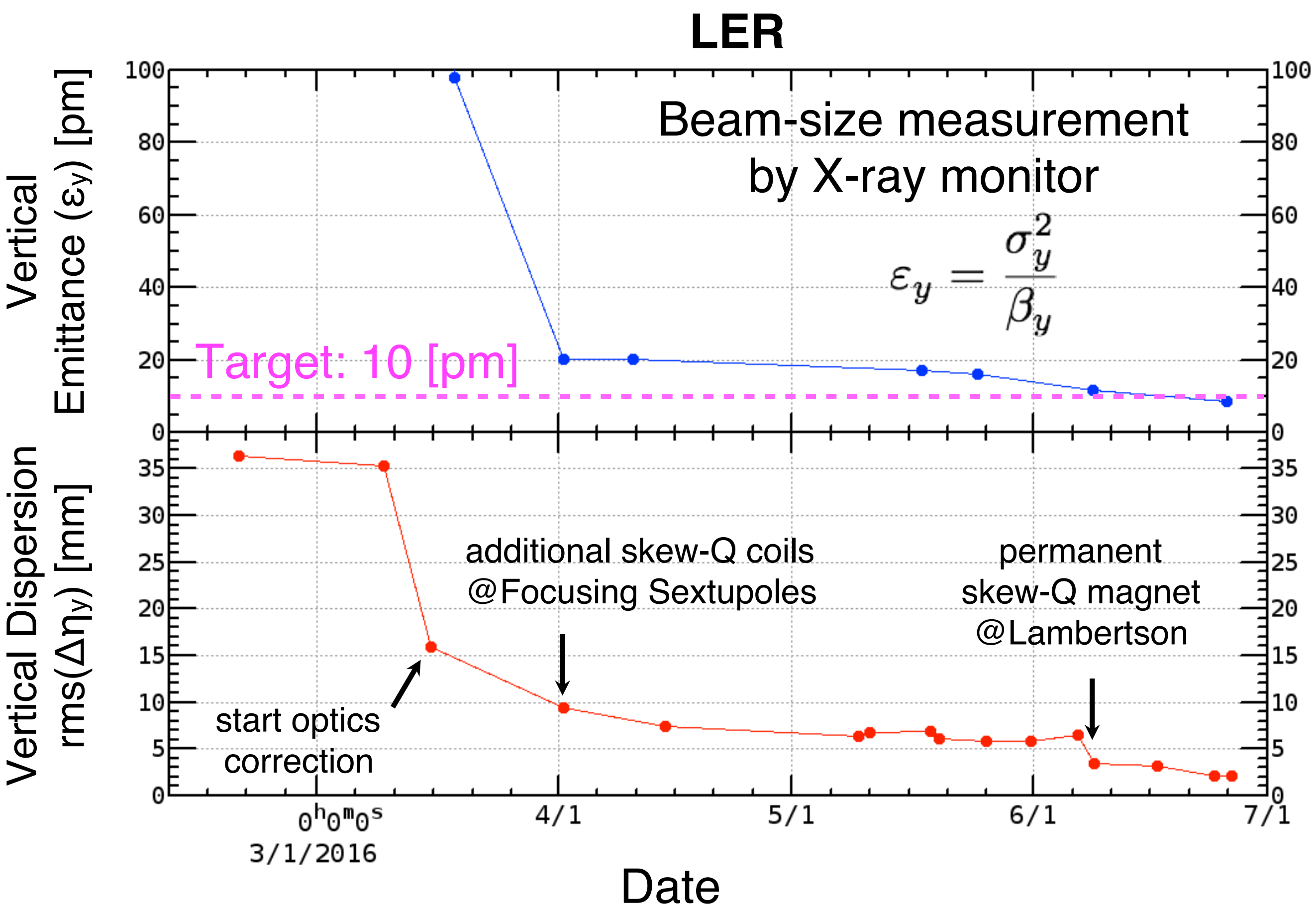

skew-Q corrector coil on sextupole

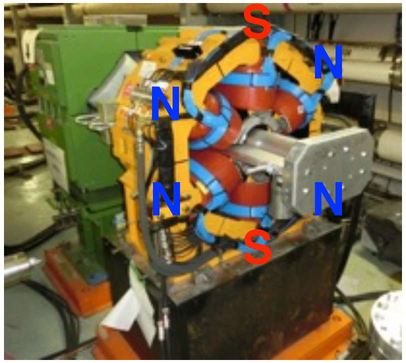

permanent skew-Q to correct error field of Lambertson

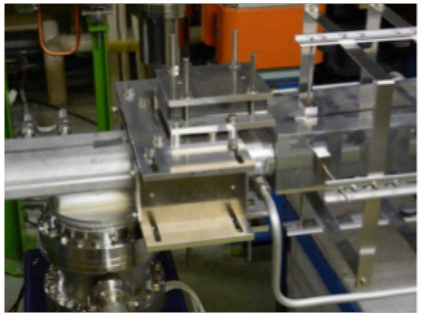

Y. Ohnishi et al.

Low Emittance Tuning

- Skew Q-like corrector windings on sextupoles are newly introduced at SuperKEKB to correct x-y couplings and vertical dispersion almost independently.
  - Vertical orbit bumps at sextupoles were used at KEKB.

Symmetric excitation localizes dispersion.

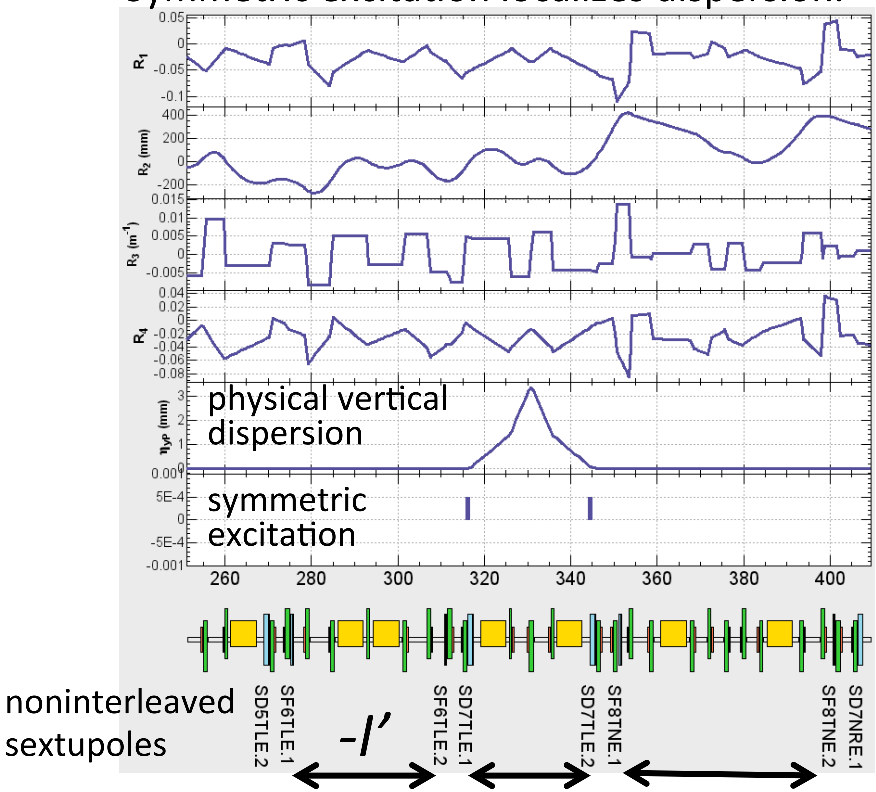

Asymmetric excitation localizes x-y couplings.

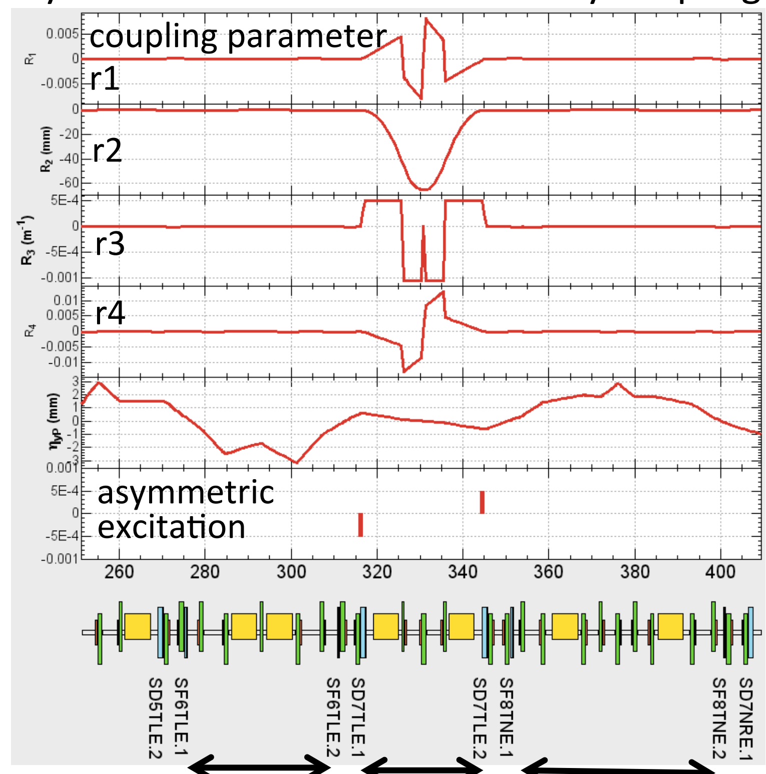

Y. Sugimoto et al.

Low Emittance Tuning

x–y coupling correction in LER

- Observables are vertical orbits excited by horizontal steering magnets.
- The vertical orbits were successfully corrected by skew-Q windings.
- Localized coupling source was also corrected by additional skew-Q correctors.

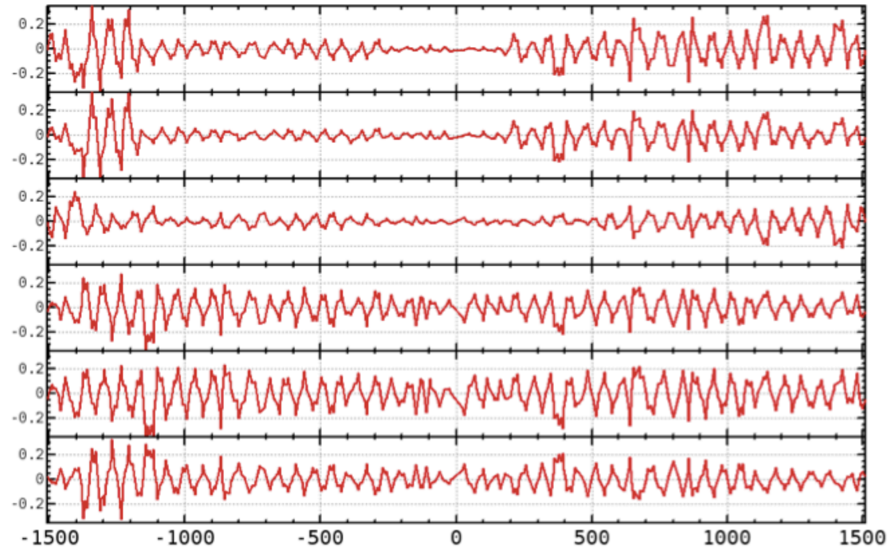

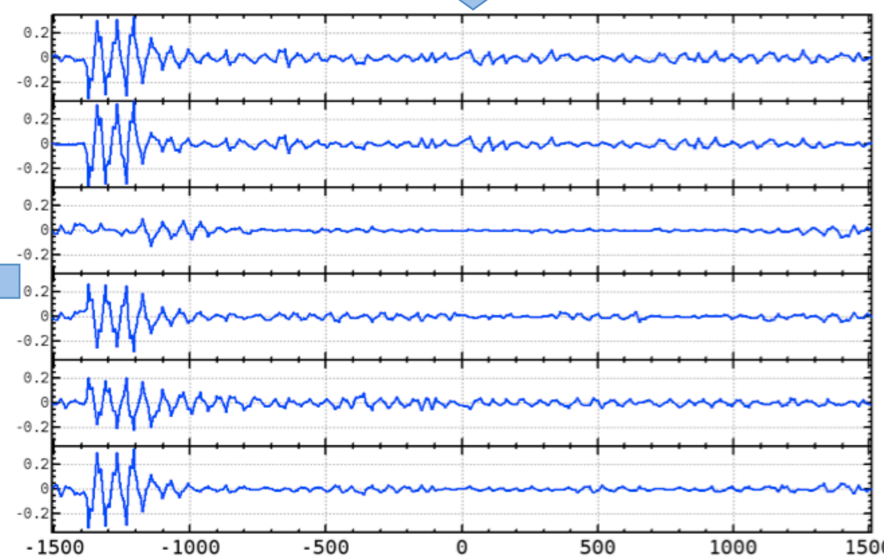

$$\Delta\tilde{y} \equiv (\Delta y)^{\mathrm{rms}} \,/\, (\Delta x)^{\mathrm{rms}}$$

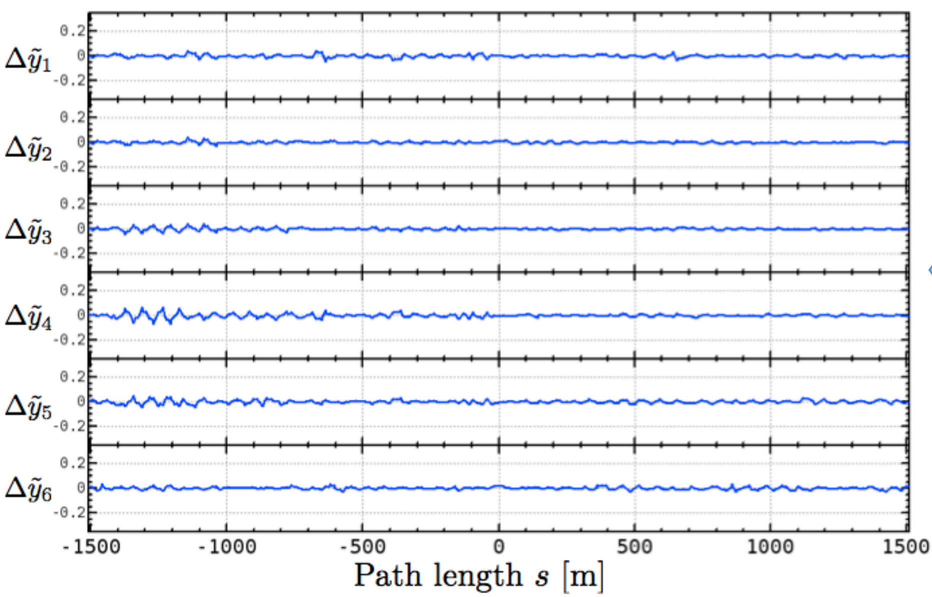

H. Sugimoto et al.

Low Emittance Tuning

- Optics correction of HER and LER is in the same level. The vertical emittance in HER is also expected to be ~10 pm.

Results of optics correction in Phase-1

Items	Symbol	LER	HER
Coupling strength	$\lvert C^{-} \rvert$ ($\times 10^{-3}$)	1.2	2.0
X-Y coupling*	rms(Δy)/rms(Δx)	0.9 %	0.6 %
Hor. dispersion	rms($\Delta\eta_x$)	8 mm	11 mm
Ver. dispersion	rms($\Delta\eta_y$)	2 mm	2 mm
Hor. β function	rms($\Delta\beta_x/\beta_x$)	3 %	3 %
Ver. β function	rms($\Delta\beta_y/\beta_y$)	3 %	3 %
Hor. tune	$\Delta\nu_x$ ($\times 10^{-4}$)	2	5
Ver. tune	$\Delta\nu_y$ ($\times 10^{-4}$)	5	1

Y. Ohnishi et al, TUT3BH, eeFACT16

Y. Ohnishi et al.

IR status for Phase-2 commissioning

Overview of the horizontal cross section of the SuperKEKB IR

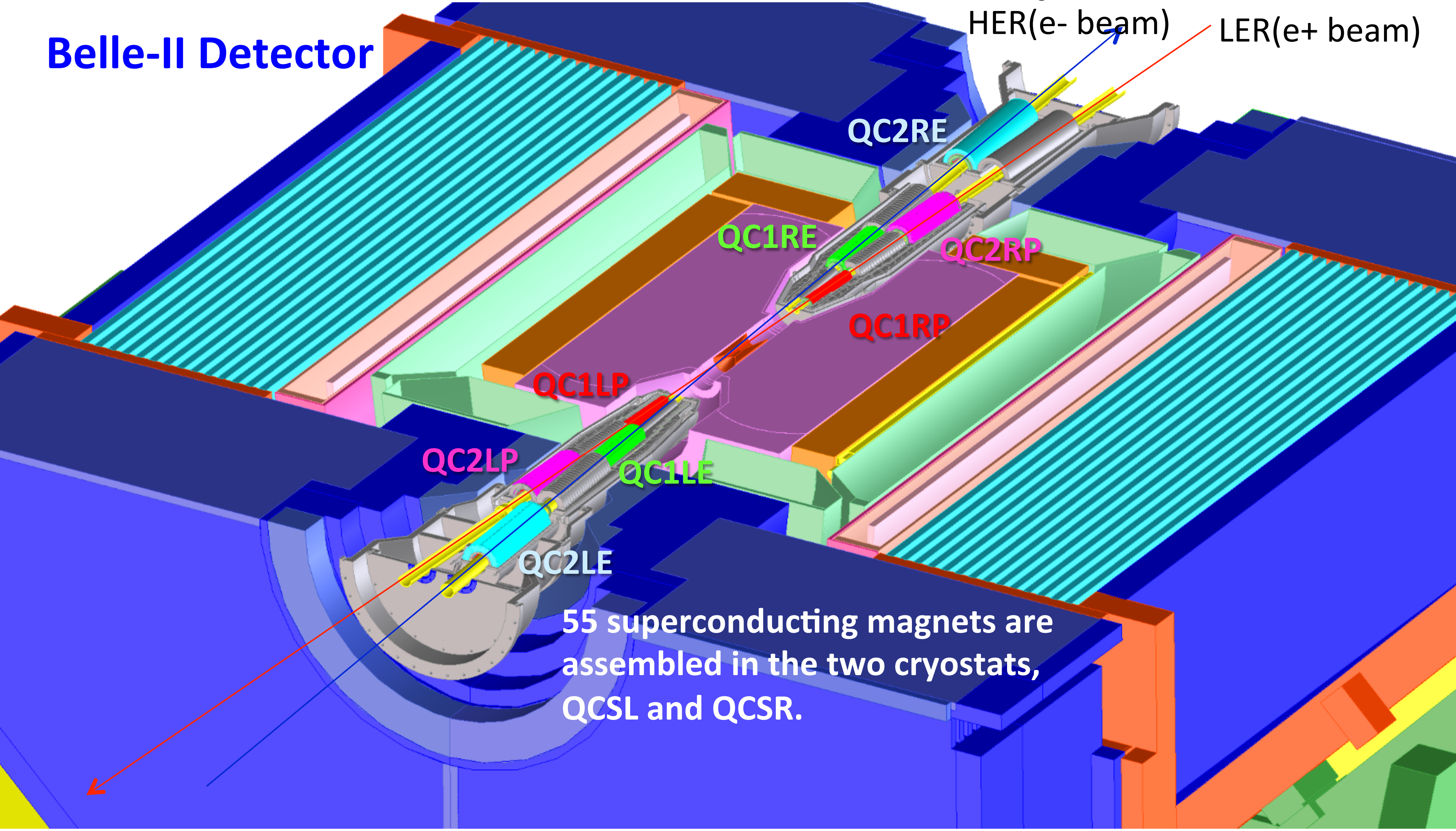

N. Ohuchi

IR status for Phase-2 commissioning

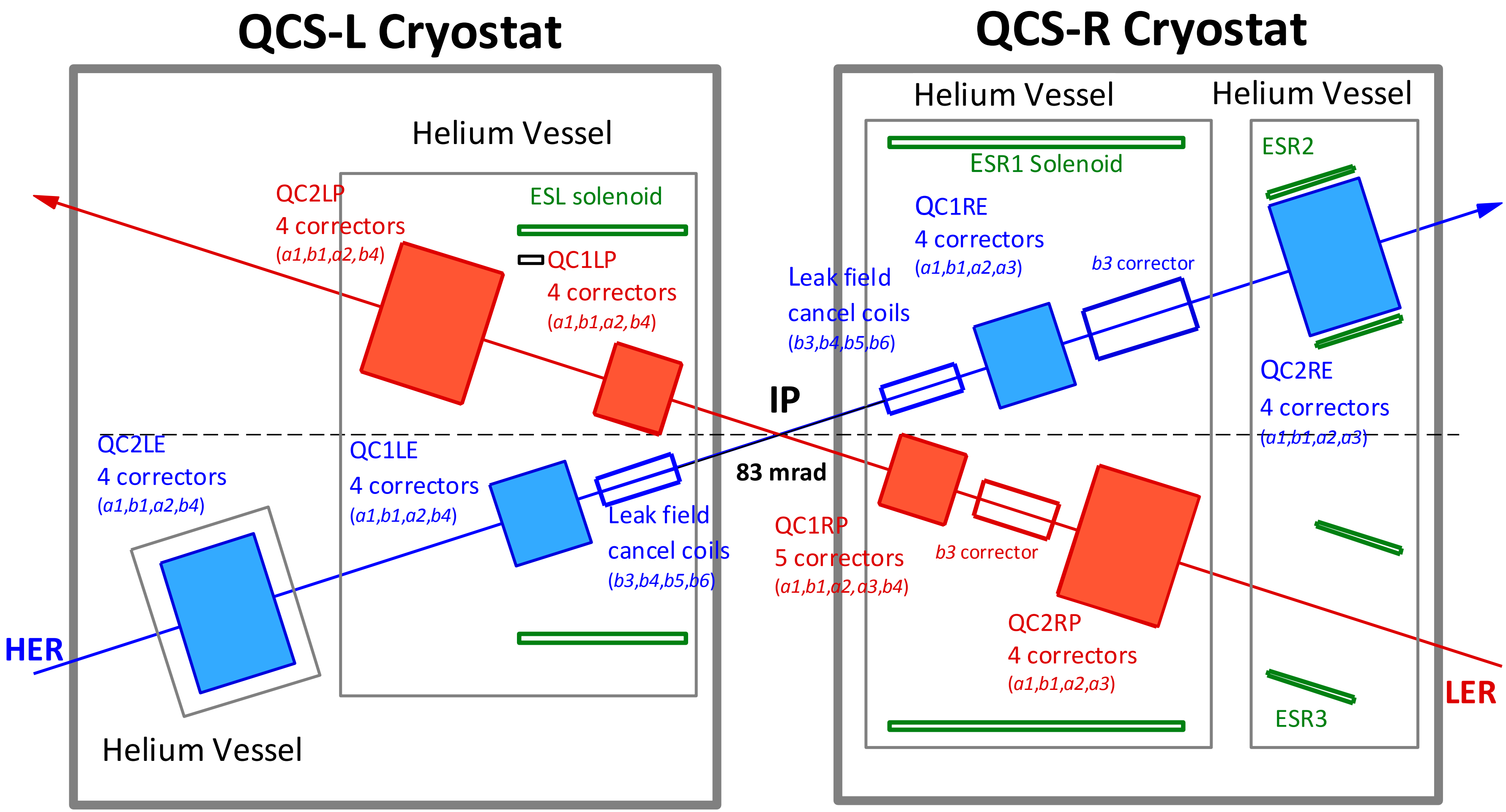

4 SC main quadrupole magnets: 1 collared magnet, 3 yoked magnets
16 SC correctors: a1, b1, a2, b4
4 SC leak field cancel magnets: b3, b4, b5, b6
1 compensation solenoid

4 SC main quadrupole magnets: 1 collared magnet, 3 yoked magnets
19 SC correctors: a1, b1, a2, a3, b3, b4
4 SC leak field cancel magnets: b3, b4, b5, b6
3 compensation solenoid

N. Ohuchi

IR status for Phase-2 commissioning

Main quadrupole magnets have the different cross section design along the beam line.

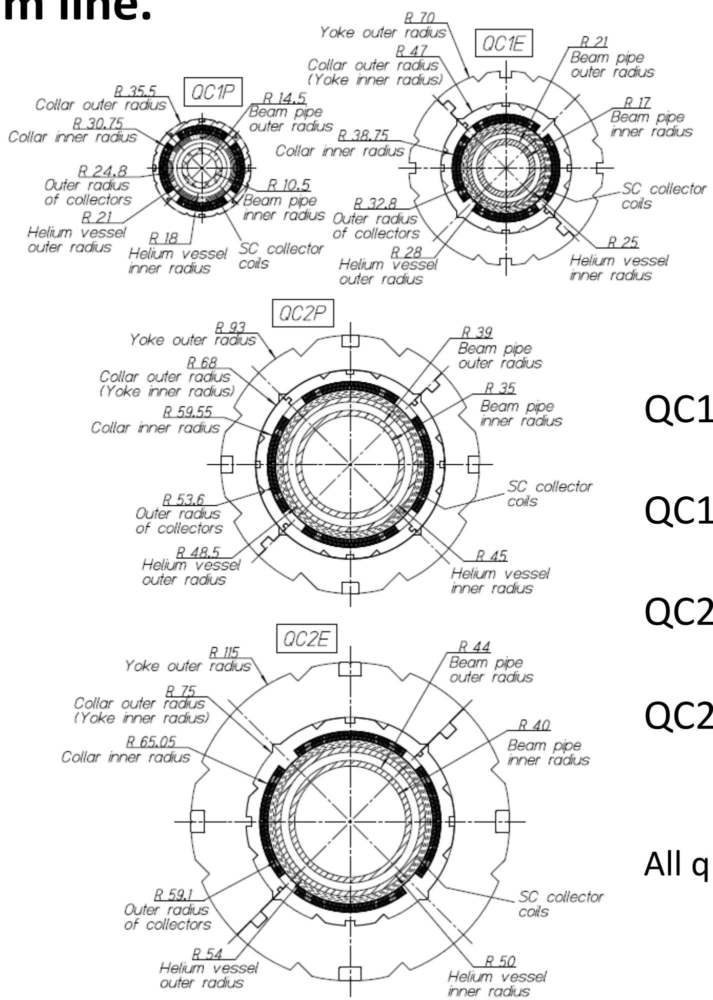

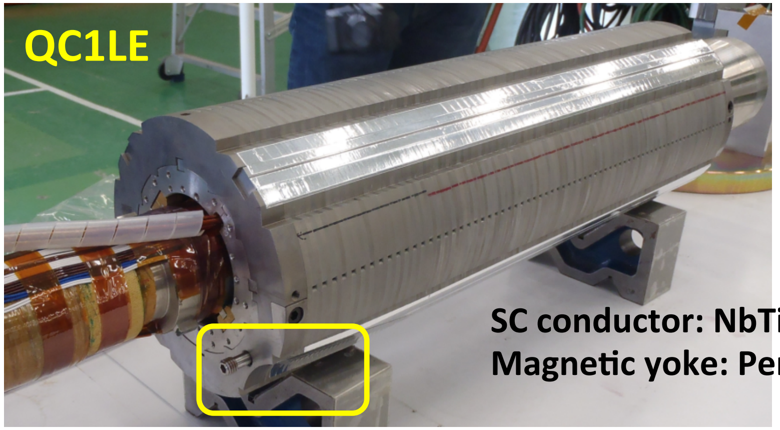

SC conductor: NbTi
Magnetic yoke: Permendur

Yokes are cut for the interference with the LER beam line.

QC1P: The quadrupole is placed at the closest position to IP for LER. Non-magnetic yoke magnet , *G*=69 T/m.
QC1E:The quadrupole is placed at the closest position to IP for HER. Yoked magnet (Permendur) , *G*=72 T/m.
QC2P: The quadrupole for LER. Yoked magnet (Permendur), SC coil thickness=5.4 mm (R_{coil}=53.7mm), *G*=28 T/m.
QC2E:The quadrupole for HER. Yoked magnet (Permendur), SC coil thickness=5.4 mm (R_{coil}=59.2mm), *G*=32 T/m.

All quadrupole magnets have the multi-layer corrector magnets.

N. Ohuchi

IR status for Phase-2 commissioning

Construction of superconducting corrector magnets

- The corrector magnets were constructed by BNL under the research collaboration
  - BNL special technique: direct winding method
  - The SC coils were wound directly on the helium inner vessel, and they are multi-layered.
  - Types of corrector magnets:
    - Normal and skew dipoles: correction of the quadrupole center magnetically
    - Skew quadrupole: correction of the quadrupole mid-plane angle
    - Normal and skew sextupoles: cancelling the sextupole fields induced by the assembly errors of the quadrupoles
    - Normal octupole: tuning the dynamic apertures
    - QC1P leak field cancel magnets (sextupole, octupole, decapole, dodecapole): cancelling the leak field from QC1P to HER beam line. QC1P is the magnet without magnetic yokes.

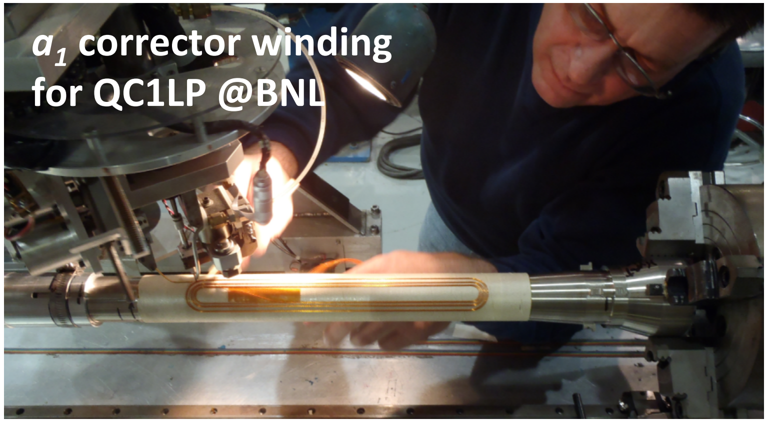

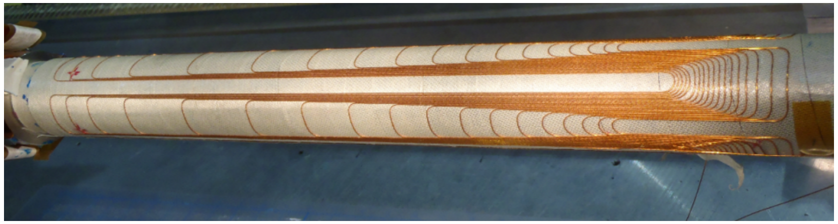

QC1P octupole leak field cancel magnet

N. Ohuchi

Construction of QCS superconducting magnets

- SC quadrupole magnets and corrector magnets
  - Three quadrupole magnets (QC1LP, QC1LE, QC2LP) and the corrector magnets were assembled in the support block to keep the precise position between magnets.

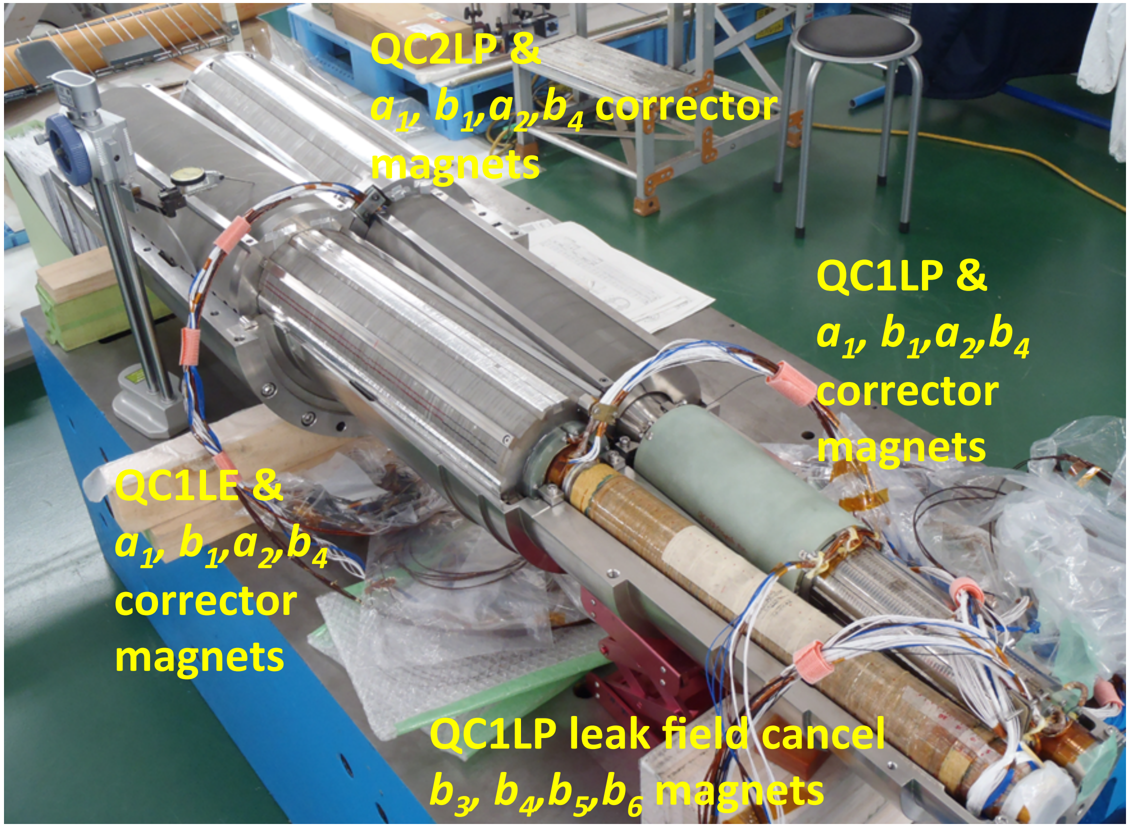

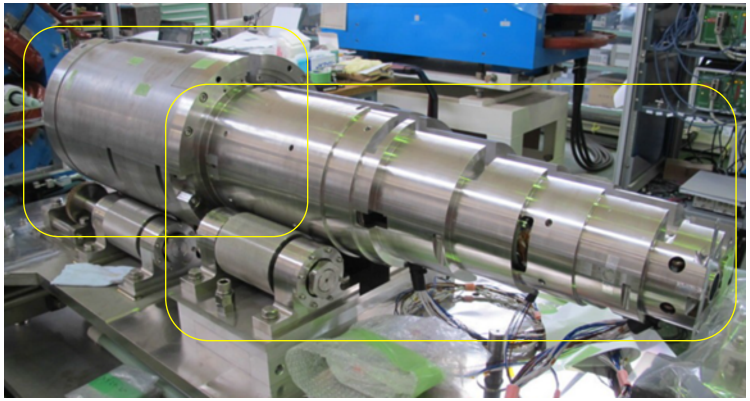

The magnets are covered with the stainless steel block and the iron block.

N. Ohuchi

IR status for Phase-2 commissioning

- Compensation solenoids [ESL, ESR1, ESR2 and ESR3]
  - Cancelling the integral solenoid field by the Belle-II solenoid on each side of IP
  - Making the optimized solenoid field profile in the area close to IP

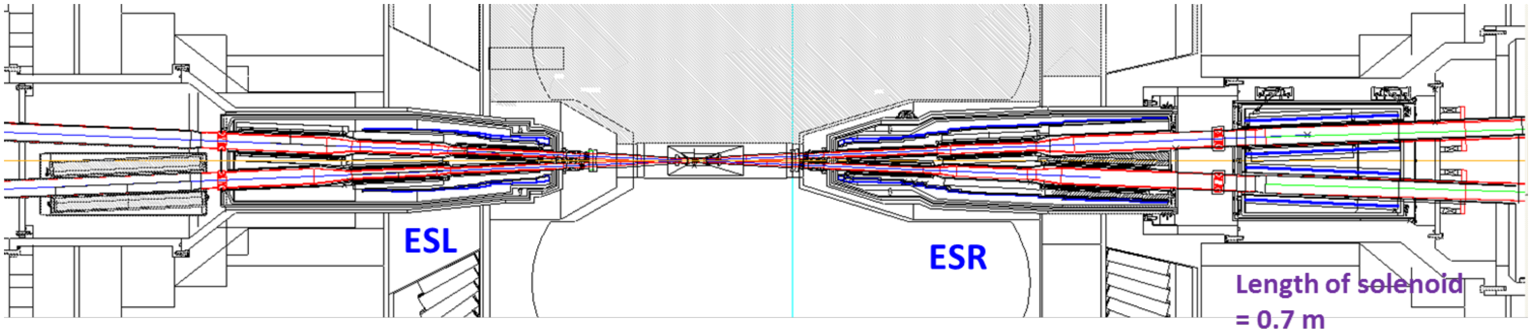

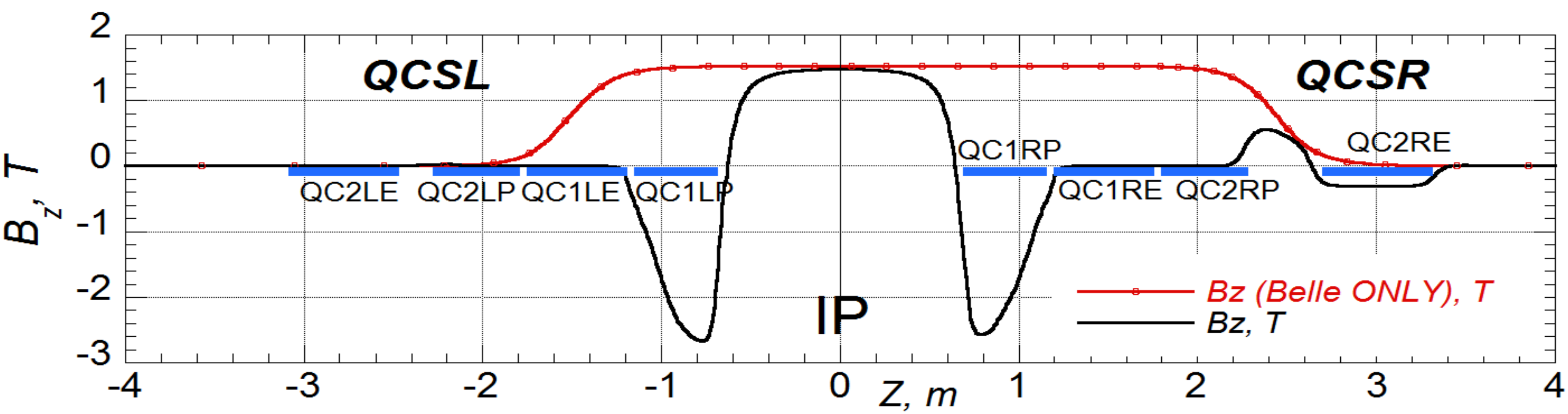

- In the left cryostat, one solenoid (12 small solenoids) is overlaid on QC1LP and QC1LE.
- In the right cryostat, the 1st solenoid (15 small solenoids) is overlaid on QC1RP, QC1RE and QC2RP.
  - The 2nd and 3rd solenoids on the each beam line in the QC2RE vessel.

N. Ohuchi

Construction of QCS superconducting magnets

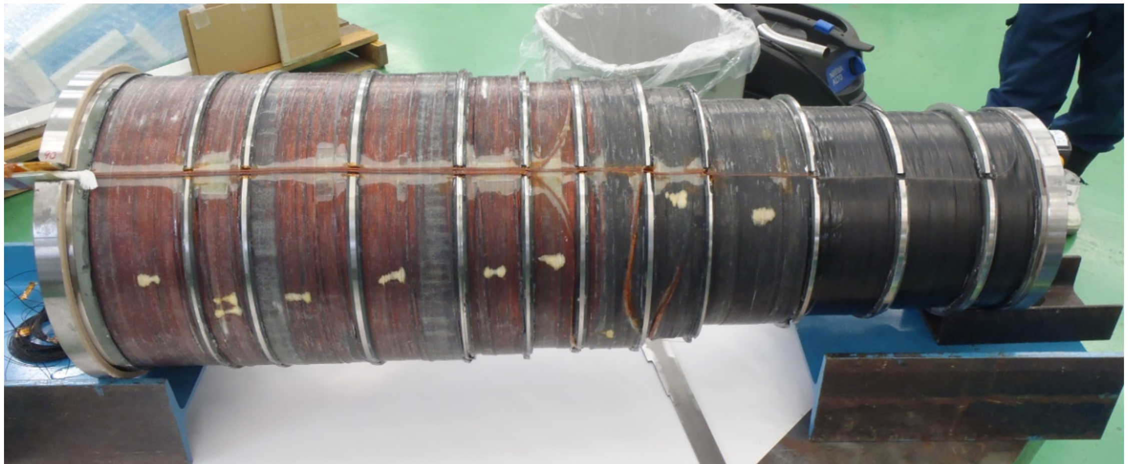

ESL consists of 12 coils:
Magnet length= 914 mm
Maximum field at 403 A= 3.53 T
Stored Energy= 118 kJ

ESR1 consists of 15 coils:
Magnet length= 1575 mm
Maximum field at 450 A=3.19 T
Stored Energy= 244 kJ
Cold diode quench protection system

N. Ohuchi

Assembly of ESR2, QC2RE and corrector magnets

Complex magnets

From inner magnet bore:

- Four-layered correctors
- Collared QC2RE
- ESR2 compensation solenoid
- Iron magnetic yokes

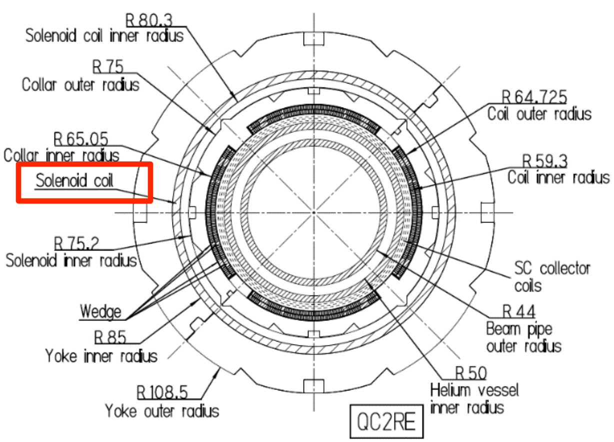

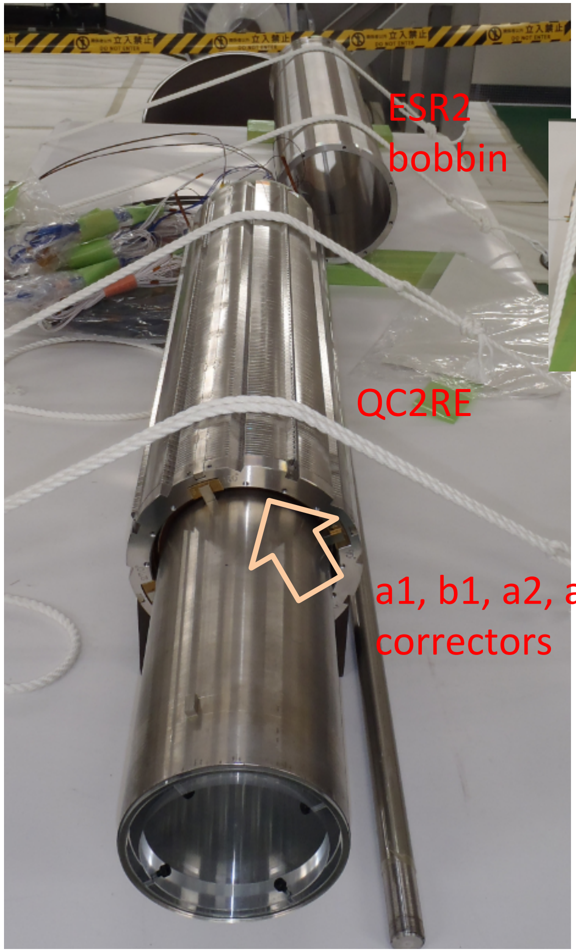

ESR2 compensation solenoid

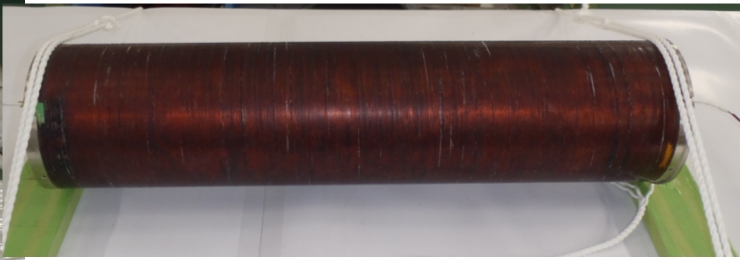

Collared QC2LE

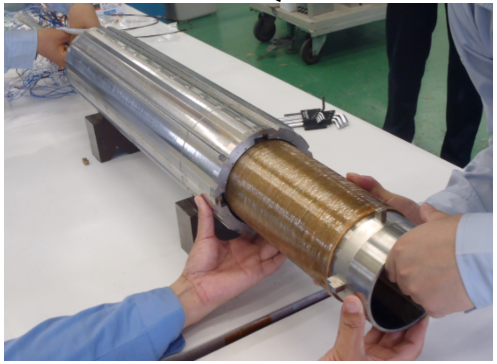

4 layer-corrector magnets

N. Ohuchi

IR status for Phase-2 commissioning

Important components for beam operation: **radiation shield**

- **Radiation shield of W-alloy is cooled to 4 K with SC magnets**

Assembled cold mass of quadrupoles and correctors for QCSL

Combination of the cold mass and the ESL solenoid

Assembling the radiation shield of **W alloy** on ESL

Covering the cold mass with the helium vessel and welding the vessels

N. Ohuchi

IR status for Phase-2 commissioning

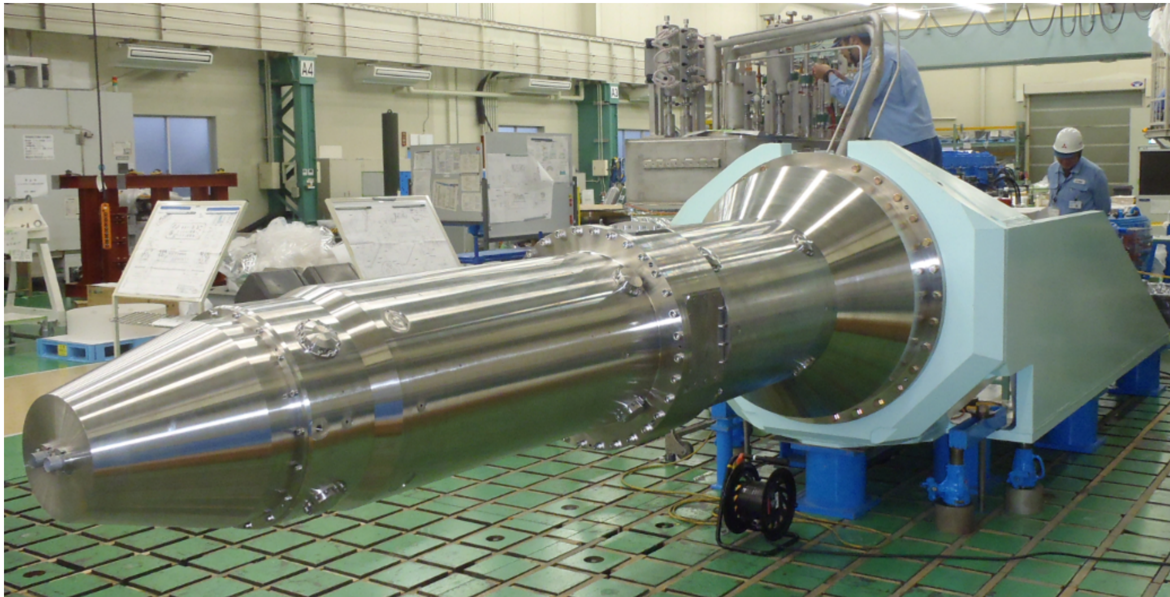

QCS-R magnet-cryostat

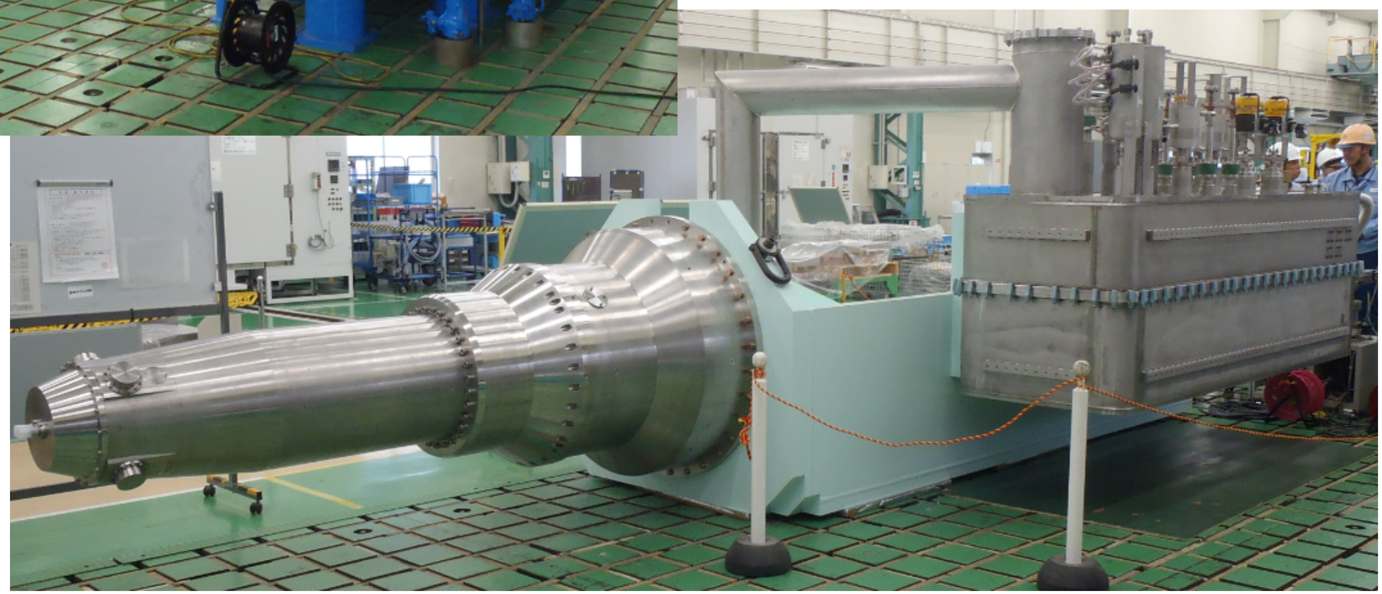

QCS-L magnet-cryostat

N. Ohuchi

IR status for Phase-2 commissioning

Construction of QCS system in SuperKEKB IR

- 25th Dec. 2015: The QCS-L cryostat was delivered to KEK
- Feb. 2016 ~ Jul. 2016: Cold tests of the QCS-L cryostat in the Experimental Laboratory
- 1st August 2016: The QCS-L cryostat was installed on the beam lines.
- 1st Sept. 2016 ~ 20th Oct. 2016: Construction work of the QCS-L cryogenic system
- 7th Nov. 2016 ~ 22nd Dec. 2016: Cold tests of the QCS-L system
- 13th Feb. 2017: QCS-R cryostat was delivered to KEK, and the cryostat was installed on the beam lines.
- March 2017: The QCS-R system has been integrated with the cryogenic system and the power supplies.
- **May - August 2017: Commissioning and field measurements of the QCS-L and QCS-R systems with exciting Belle-II solenoid**

N. Ohuchi

IR status for Phase-2 commissioning

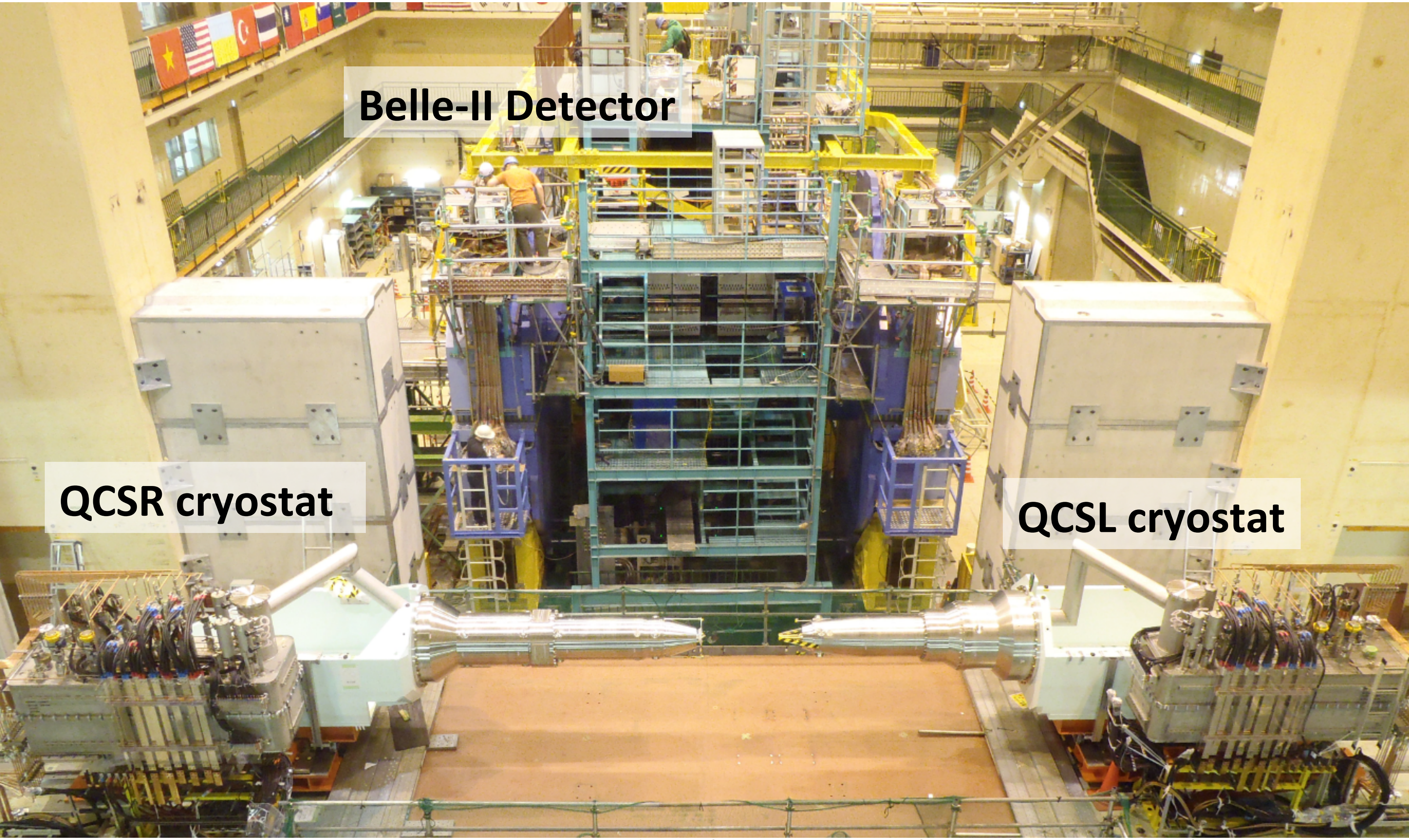

Two magnet cryostats were integrated on the SuperKEKB beam lines in March 2017.

N. Ohuchi

IR status for Phase-2 commissioning

The Belle-II particle detector was rolled in the SuperKEKB Interaction Region on April 11th, 2017.

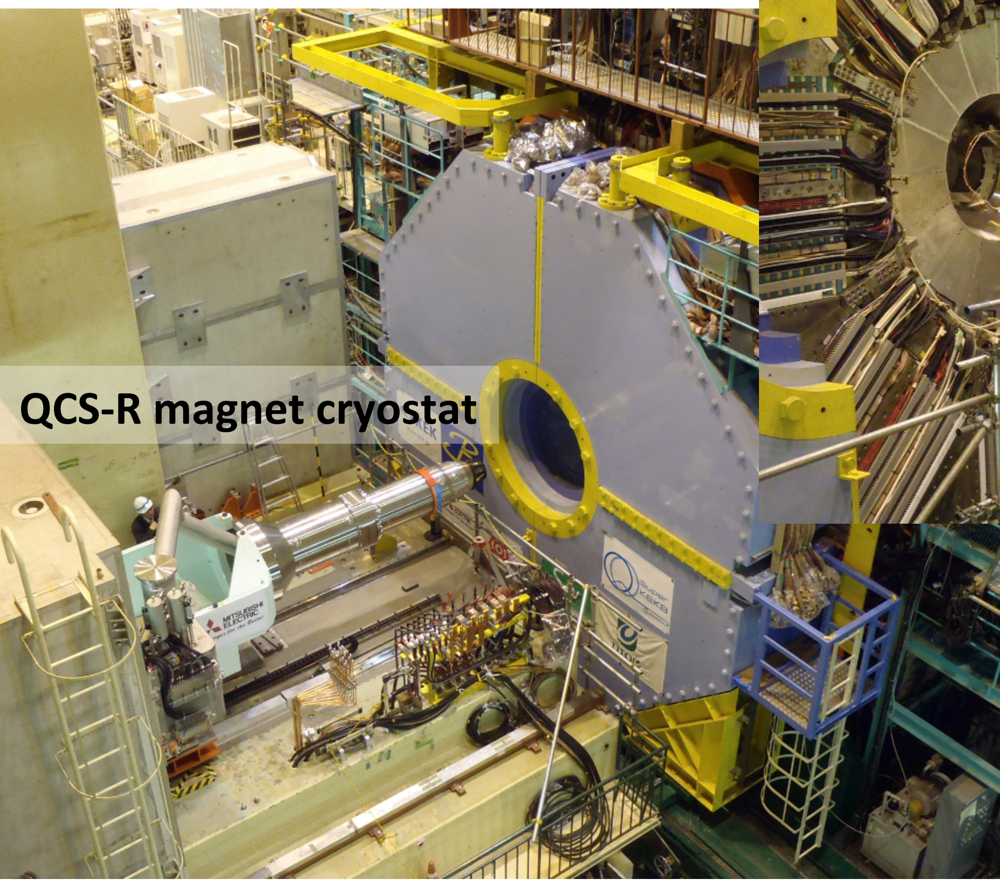

QCS-R magnet cryostat

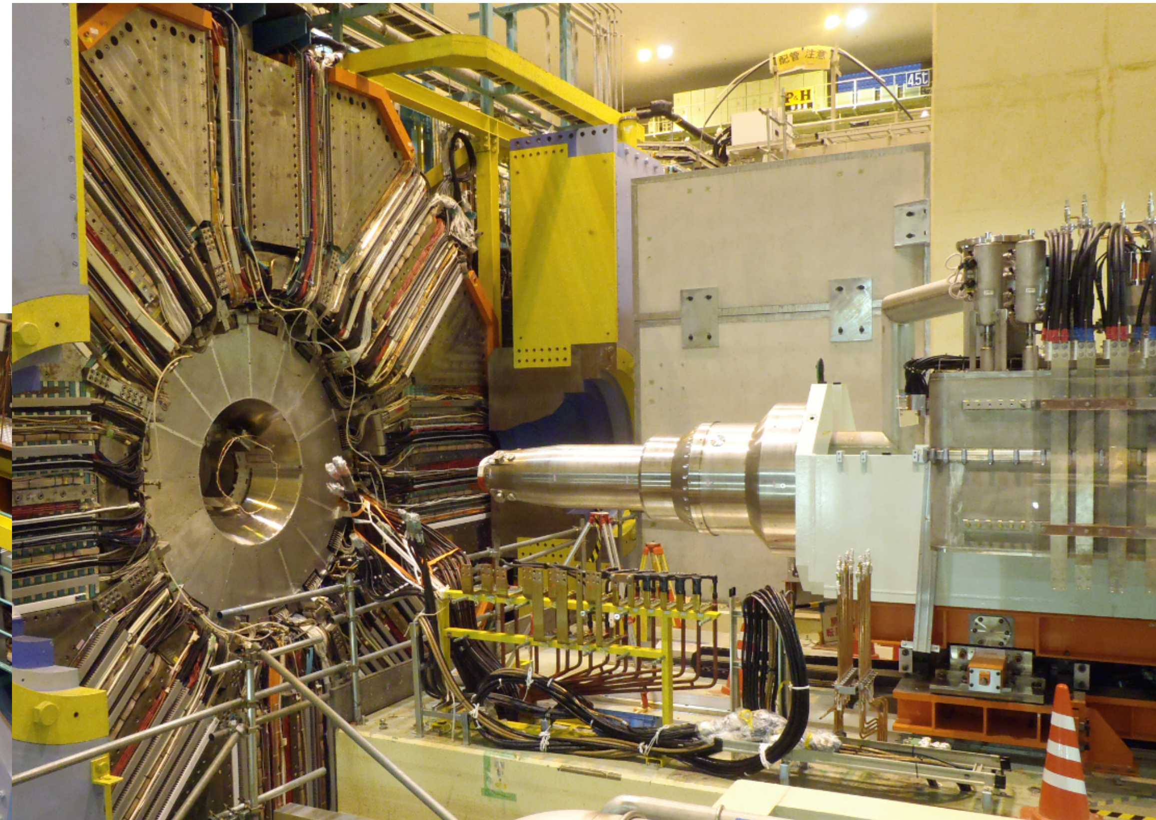

QCS-L magnet cryostat

N. Ohuchi

IR status for Phase-2 commissioning

QCS-L and QCS-R were placed in the normal positions in Belle II on May 8.

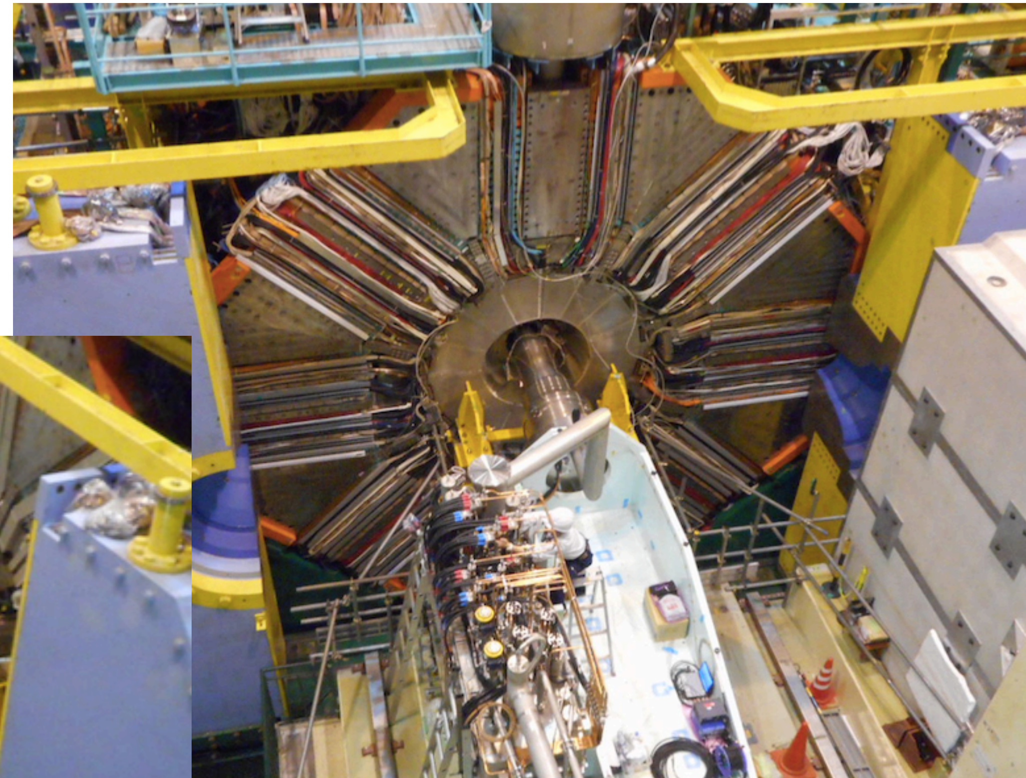

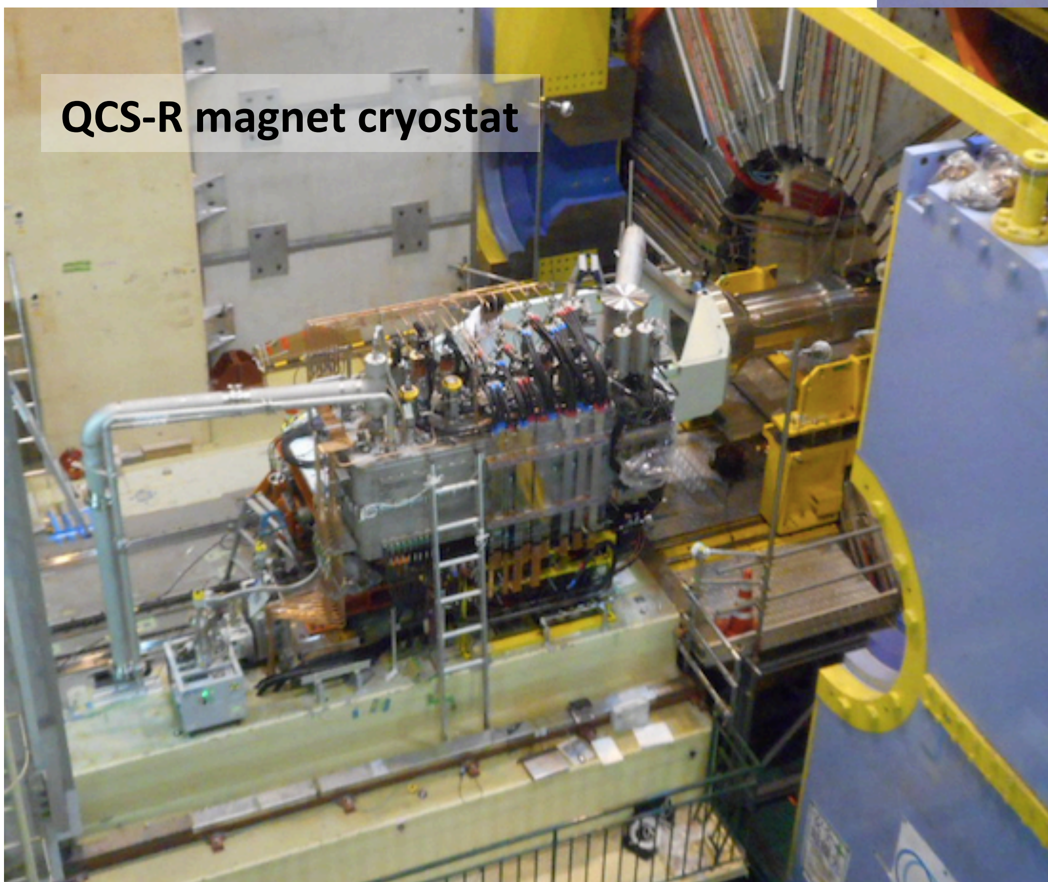

QCS-L magnet cryostat

N. Ohuchi, M. masuzawa et al.

IR status for Phase-2 commissioning

- The construction of the QCS cryostats was completed, and two cryostats and the cryogenic systems were integrated in the SuperKEKB IR in March 2017.
- The Belle II detector was rolled in on 11th April, 2017.
- Commissioning and field measurements of the QCS-L and QCS-R systems with the Belle solenoid field are scheduled from May to August, 2017, and the field parameters of the magnets for the beam operation will be measured.

Injector Complex

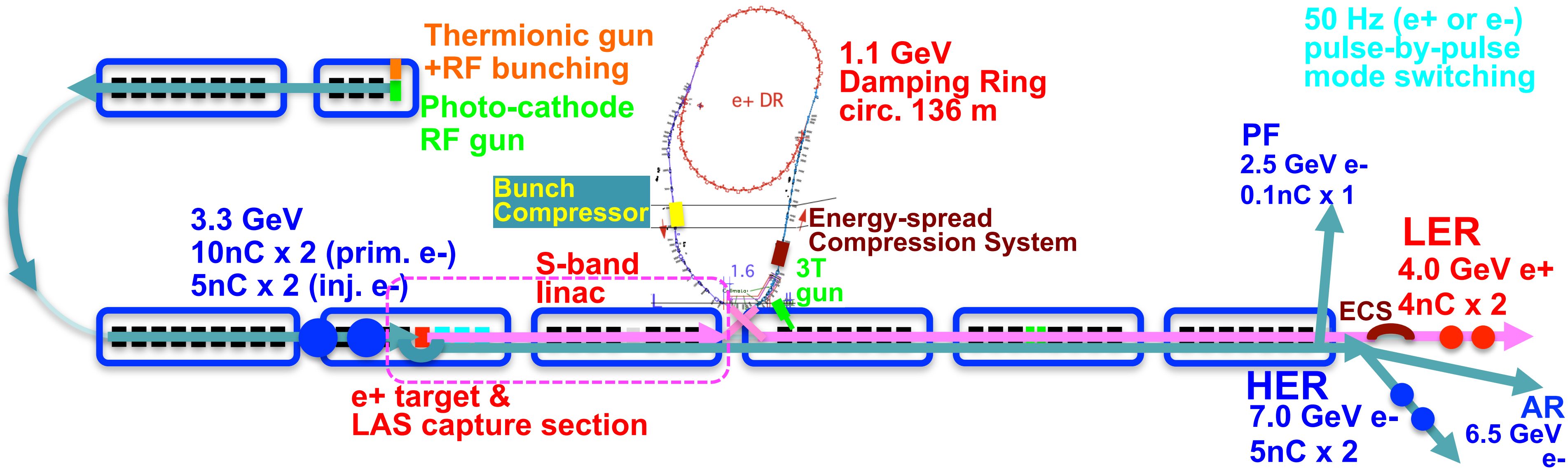

Major upgrades of injector LINAC

- Low emittance e- beam from Photo-cathode RF-gun
- High current e- beam from thermionic e-gun to generate e+
- Low emittance e+ beam with new Damping Ring
- Higher intensity of e+ beam by upgrading of e+ generator
  - Flux Concentrator, Large Aperture Structure, Solenoid Section, ~100 Quads
- Fast switching of beam optics/orbit by introducing ~70 pulsed magnets
- Higher resolution of Beam Position Monitors
- Higher accuracy of Beam line alignment

e- RF-gun unit

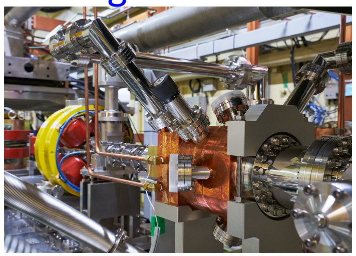

e+ generator

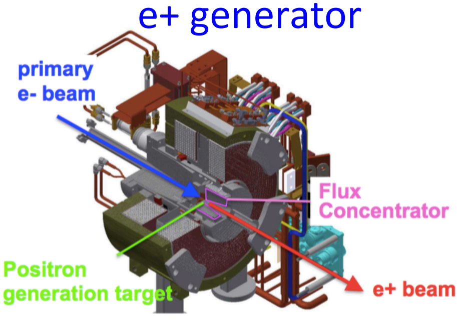

K. Furukawa et al.

Positron Damping Ring

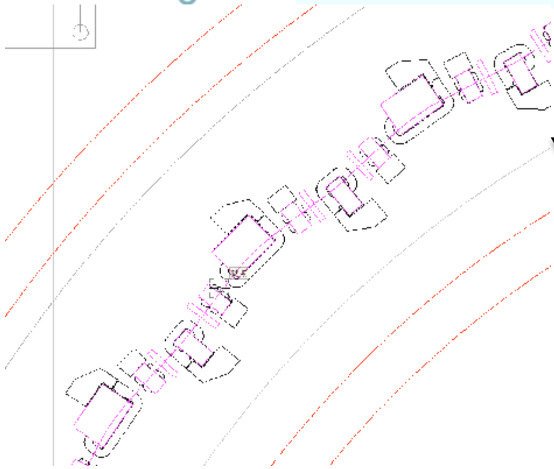

Reverse bend FODO
for short damping time

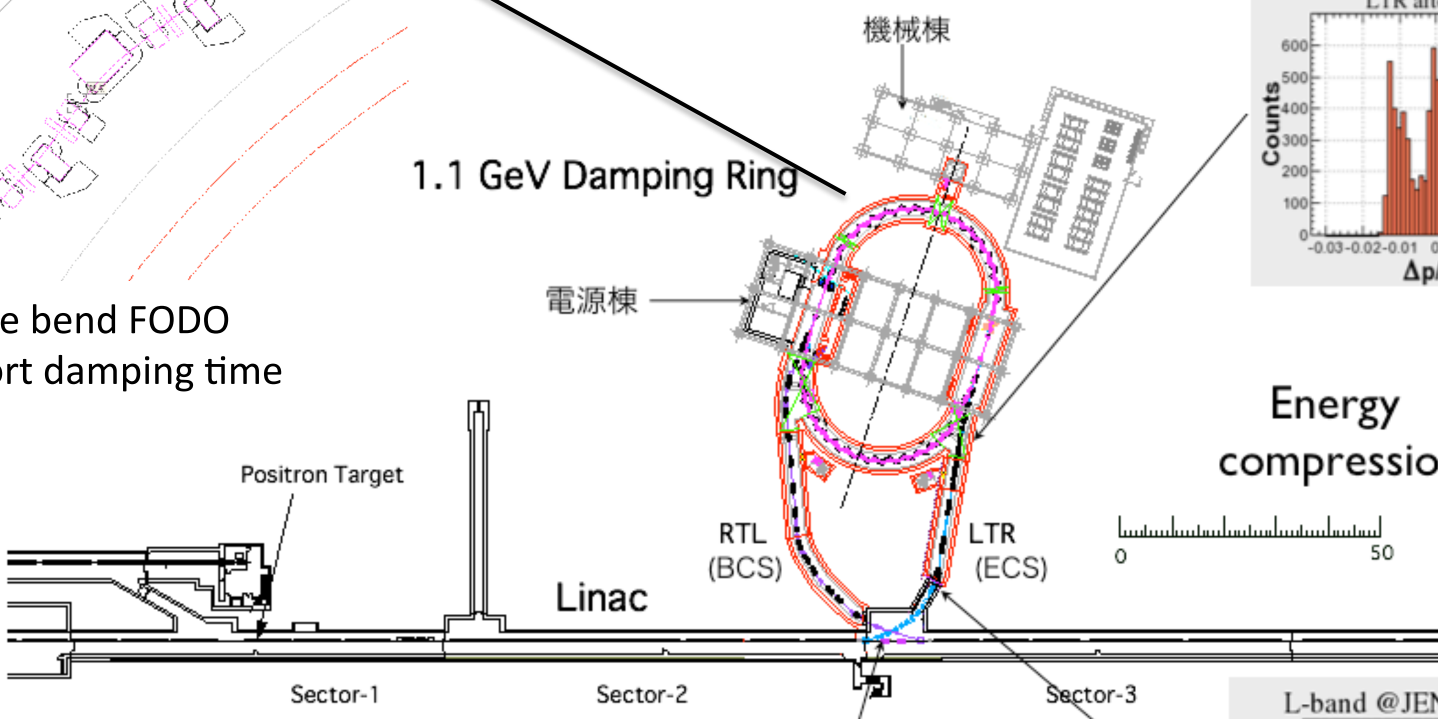

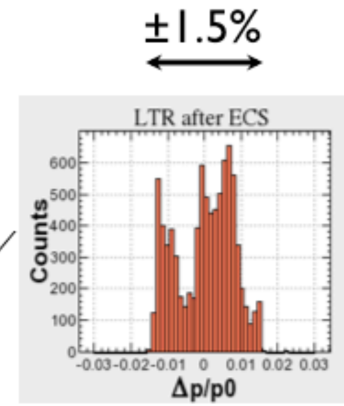

Energy
compression

Collimators in the arc
20% is cut at the tail

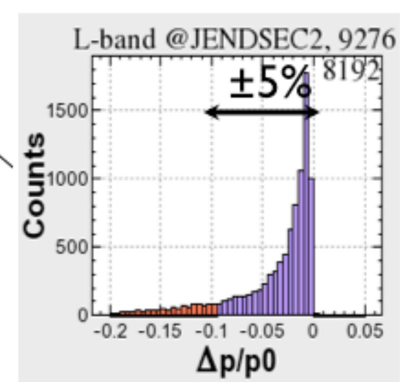

M. Kikuchi et al.

Positron Damping Ring

Table 3: Parameters of the Damping Ring

Energy		1.1		GeV
Number of bunch trains		2		
Number of bunches / train		2		
Circumference		135.498295		m
Maximum stored current		70.8		mA
Energy loss per turn		0.0847		MV
Horizontal damping time		11.57		ms
Injected-beam emittance		1400		nm
Equilibrium emittance (h/v)		41.5 / 2.08		nm
Coupling		5		%
Emittance at extraction (h/v)		42.9 / 3.61		nm
Cavity voltage	0.5	1.0	1.4	MV
Bucket height	0.81	1.24	1.5	%
Energy spread		5.5×10^{-4}		
Synchrotron tune	0.0152	0.0217	0.0257	
Equilibrium bunch-length	11.07	7.79	6.58	mm
Phase advance/cell (h/v)		64.39 / 64.64		deg
Momentum compaction factor		0.0142		
Bend-angle ratio		0.35		
Bend radius		2.7		m
Number of normal-cells		40		
RF frequency		509		MHz
Chamber size(normal cell)		$34^H \times 24^V$ w/ antechamber		mm

M. Kikuchi et al.

Positron Damping Ring

Year	Month			Status
2012	Dec.	Tunnel construction completed.		done
2013	Nov.	Power supply building construction completed.		done
2014	Mar.	Facility building construction completed.		done
2014	May – Dec.	1st period of installation	Power cables, a part of BT magnets	done
2015	May – Dec.	2nd period of installation	Mangets, Power supplies for magnets, High power RF system, BPM cables, etc.	done
2016	Jan. ～	3rd period of installation	Beam pipes, RF cavities, cooling channels, etc.	done
2017	Jan. ～	4th period of installation	ECS, BCS, Septums, Kickers, Monitors, etc.	ongoing
2017	Nov./Dec. ～	Beam commissioning starts		

M. Kikuchi, K. Akai et al.

Installation RF cavities to the DR Tunnel

(November, 2016)

T. Abe et al.

Now waiting for high-power RF conditioning* for DR operation

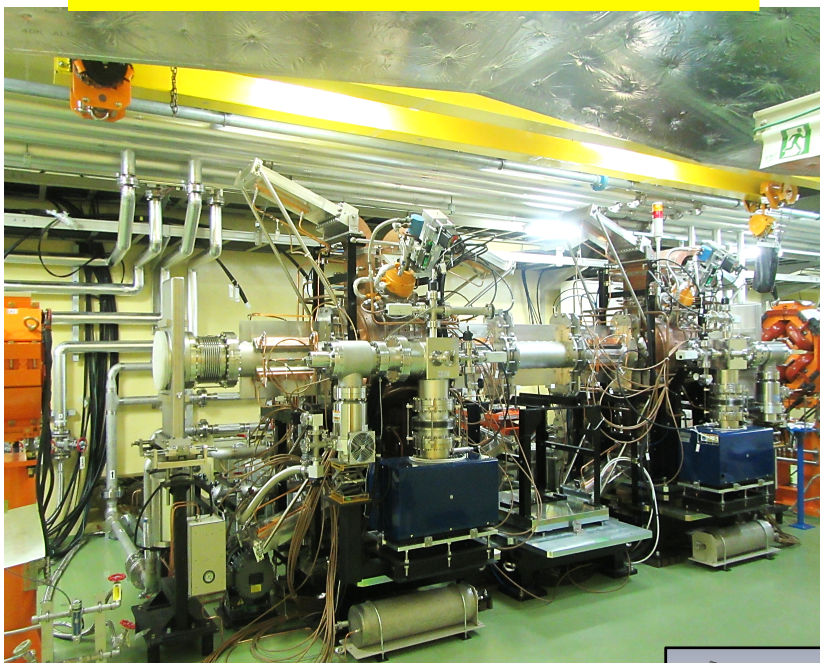

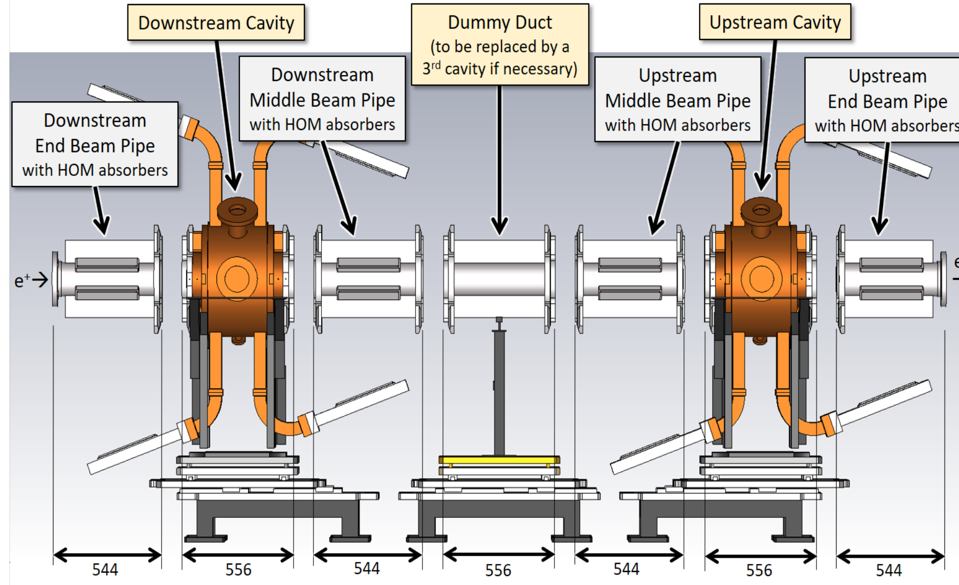

7 components aligned and solidly connected

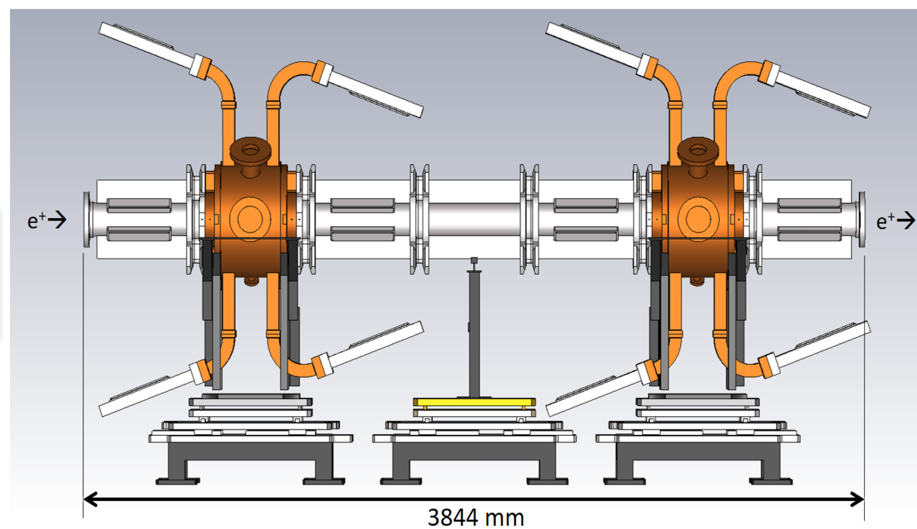

Into one big mechanical structure

* High-power RF conditioning was completed at a test stand for each cavity.

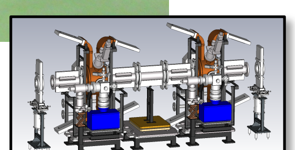

Positron Damping Ring

Installation phase-4
Beam pipes (ring) and vacuum pumps
Magnets alignment (coarse)
Cooling channels for magnets
Beam pipes at BT and Linac side
Installation of ECS and BCS cavities and waveguides
Installation of septums and kickers
Magnets alignment (fine)
Adjustment of power supplies
High power RF cavity conditioning
High power conditioning of ECS and BCS accelerating units
Evacuation of beam pipes

Arc cells of DR

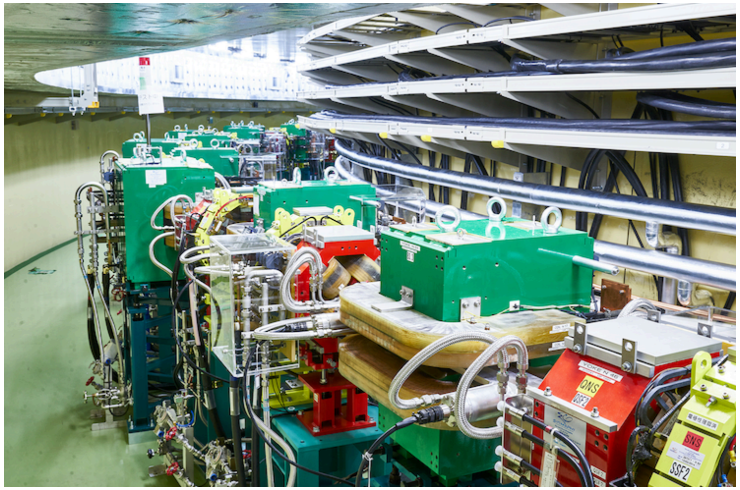

DR and the extraction line

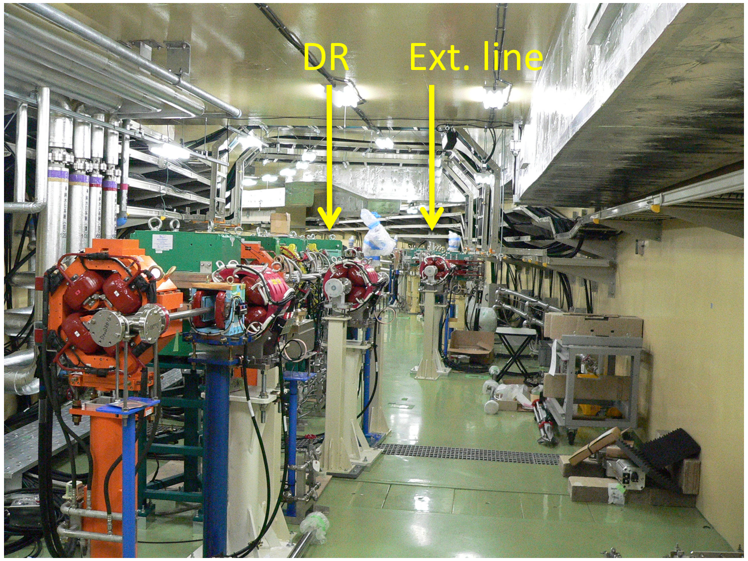

RF system tuning with cavities started in Feb. 1.

M. Kikuchi, K. Akai et al.

Schedule

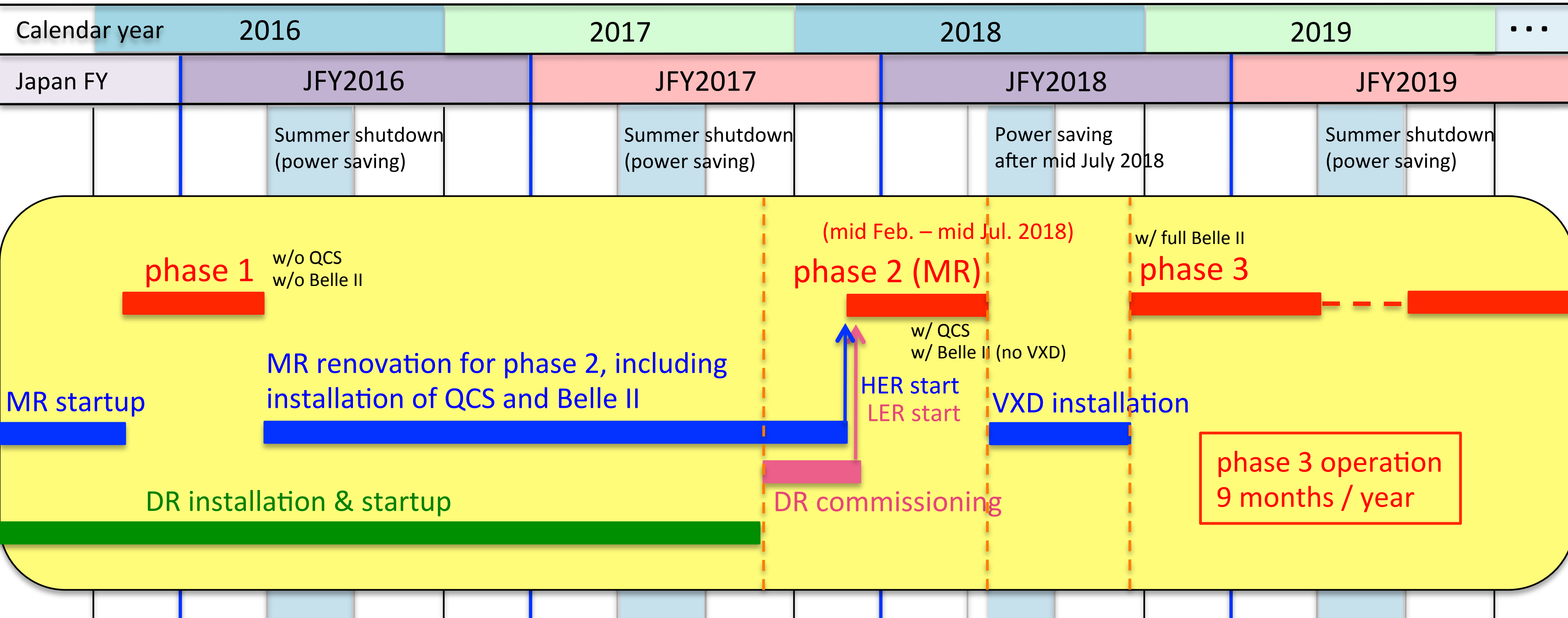

K. Akai

We are here.

Summary

- The Phase-1 commissioning of SuperKEKB collider rings was performed successfully.
  - Integrated beam currents sufficient for Belle II roll-in were achieved.
  - Electron cloud effects are not so different from expectation. Permanent magnets will be attached in drift spaces in LER.
- Renovation works for Phase-2 are steadily in progress.
  - QCS and Belle II are installed in the IR.
- The phase-2 commissioning will start:
  - positron damping ring : late 2017
  - collider rings with QCS and Belle-II : mid. Feb. in 2018

Please visit posters in this conference:

MOPAB027 Preparation of CVD Diamond Detector for fast Luminosity Monitoring of SuperKEKB
TUPAB004 Progress of 7-GeVSuperKEKB Injector Upgrade and Beam Commissioning
TUPAB005 Investigation of Beam Variation and Emittance Growth Simulation With Both Misalignments and the Beam Jitter for SuperKEKB Injector Linac
TUPAB056 New Achievements of the Laser System for RF-Gun at SuperKEKB Injector
TUPIK059 Recent progress of Dithering System at SuperKEKB
WEPIK006 Cancellation of the Leak Field from Lambertson Septum in the Beam Abort System of SuperKEKB
WEPIK007 Optics Design and Observation for the Beam Abort System in SuperKEKB HER
WEPIK009 Collimators for SuperKEKB Main Ring
WEPIK011 Ceramic Chamber Used in SuperKEKB High Energy Ring Beam Abort System
WEPIK012 Performance of SuperKEKB High Energy Ring Beam Abort System
WEPIK013 Construction of New Septum Magnets for SuperKEKB Electron Ring Injection
WEPIK075 Electron Cloud Instability in SuperKEKB Phase I Commissioning
WEPVA055 Pre Orbit Correction Based on Tunnel Level Measurement in SuperKEKB
WEPVA058 Development of HOM Absorber for SuperKEKB
THPAB021 Coherent Beam-Beam Instability in Collision With a Large Crossing Angle
THPAB022 Ion Instability in SuperKEKB
THPAB113 Time Synchronization for Distant IOCs of the SuperKEKB Accelerators
THPAB114 Operation of LLRF Control Systems in SuperKEKB Phase-1 Commissioning
THPAB115 Development of a Longitudinal Feedback System for Coupled Bunch Instabilities Caused by the Accelerating Mode at Superkekb
THPVA012 Transverse Impedance Measurement in SuperKEKB
THPVA047 Developing an Yb/Nd Doped Hybrid Solid Laser of RF Gun for SuperKEKB Phase II Commissioning

Thank you for your attention.